

MAGNETIC RESONANCE AND RELATED STUDIES IN SOME CERIUM AND SAMARIUM COMPOUNDS

S. K. MALIK and R. VIJAYARAGHAVAN

*Tata Institute of Fundamental Research,
Homi Bhabha Road, Bombay-400005, India*

and

S. K. GARG and R. J. RIPMEESTER

National Research Council, Ottawa, Canada

ABSTRACT

The results of nuclear magnetic resonance (n.m.r.) and susceptibility measurements in CePt_2 , CePt_5 and CeSn_3 are presented together with other available results on these compounds. The magnetic susceptibility of both CePt_2 and CePt_5 can be understood on the basis of the crystal field splitting of the ground level of Ce^{3+} ion. There are two non-equivalent Pt sites in CePt_5 and, consequently, two ^{195}Pt n.m.r. lines with different Knight shifts have been observed. The ^{195}Pt Knight shifts in CePt_2 and CePt_5 are proportional to the corresponding bulk susceptibilities in the temperature region 100–300 K. However, the ^{195}Pt Knight shifts for the two Pt sites in CePt_5 behave anomalously relative to the corresponding Knight shifts in PrPt_5 and NdPt_5 . The magnetic susceptibility of CeSn_3 shows a broad maximum around 135 K and a rapid rise below 30 K. The ^{119}Sn Knight shift in CeSn_3 in the temperature region 1.2–300 K is not proportional to the bulk susceptibility. The electrical resistivity of CeSn_3 shows a T^2 term at low temperatures and the coefficient of the electronic specific heat is also very large. These results suggest sizeable 4f occupation near the Fermi level in CeSn_3 .

In samarium compounds, the 4f contribution to the Knight shift of the non-magnetic constituent is expected to cross over (or pass through zero) at a temperature of about 300 K, called the crossover temperature (T_{co}). Though this has been observed in many samarium compounds, the crossover in the Knight shifts is absent from SmSn_3 , SmAl_2 and SmF_3 , while $T_{\text{co}} = 230$ K in SmPt_2 . It is shown that because of the mixing of the excited J levels of Sm^{3+} ion into its ground level by crystal fields, the crossover temperature may be considerably reduced from the value of 300 K in free Sm^{3+} ion or crossover completely suppressed. The crystal field effects on other magnetic properties of Sm^{3+} ion are also discussed. The crystal fields may introduce one or more crossover(s) in the 4f-induced hyperfine field (H_{4f}/H) at a samarium nuclear site in the paramagnetic state while H_{4f}/H is positive throughout for free Sm^{3+} ion. In ferromagnetic compounds the crystal fields may reduce or enhance the magnetic moment of Sm^{3+} ion (compared to free ion value) and in some cases Sm^{3+} ion behaves effectively like an ($L + S$) ion rather than an ($L - S$) ion. Moreover, the Sm^{3+} magnetization also shows a crossover, the temperature of which depends on the crystal fields.

I. GENERAL INTRODUCTION

The rare earths, or the lanthanides, are characterized by the progressive filling of the 4f shell of their electronic configurations. The f electrons are responsible for the magnetic and spectroscopic properties of rare earth ions. The metallic rare earth systems (with certain exceptions) can be considered as an assembly of tripositive ions embedded in a sea of conduction electrons. The mean radius of the 4f shell is very small compared to the interionic spacing between the rare earth ions, so that the overlap between the f orbitals centred on adjacent ions is negligible. In spite of this fact the rare earth compounds are known to order magnetically, sometimes with fairly high Curie or Néel temperatures. The relatively strong magnetic coupling between rare earth ions is thought to arise from an indirect exchange interaction involving the conduction electrons. The theory of the indirect exchange interaction was developed by Ruderman and Kittel¹, Kasuya² and Yosida³. According to this theory which is now usually referred to as Ruderman–Kittel–Kasuya–Yosida (RKKY) theory, there is an exchange interaction between the conduction spins s and the localized 4f spins S given by the Hamiltonian

$$\mathcal{H} = - J_{\text{sf}} \mathbf{S} \cdot \mathbf{s} = - 2J(0) \mathbf{S} \cdot \mathbf{s} \quad (1)$$

where J_{sf} [or $J(0)$] is the effective exchange integral. Such an interaction causes a long range oscillatory polarization of conduction electron spins, which, apart from providing an effective coupling between the rare earth ions, also gives rise to an excess Knight shift at the non-magnetic site and a paramagnetic g shift of the rare earth ion. According to RKKY theory the excess Knight shift $K_f(T)$ due to the presence of 4f electron spins is given by

$$K_f(T) = K_0 [6\pi Z J(0) \langle S_z \rangle_{\text{av}} / \mu_B H] \sum_n F(2k_F R_n) \quad (2)$$

where K_0 is the Knight shift due to Pauli paramagnetism only, Z is the average number of conduction electrons per atom, $J(0)$ is the $q = 0$ value of the exchange constant, k_F is the Fermi wave vector, $\langle S_z \rangle_{\text{av}}$ is the thermal average of the z -component of the rare earth spin. The function $F(x)$ stands for

$$F(x) = (x \cos x - \sin x) / x^4 \quad (3)$$

where $x = 2k_F R$, and R_n is the distance of the n th rare earth from the resonant nucleus under consideration. The summation in equation 2 is over all the rare earth ions. The total Knight shift is given by $K(T) = K_0 + K_f(T)$.

In the model used by Jaccarino⁴, the conduction electron polarization is assumed to be uniform and the resulting Knight shift is given by

$$K_f(T) = -K_0 J_{\text{sf}} \langle S_z \rangle_{\text{av}} / 2\mu_B H \quad (4)$$

In general, if the interaction between the nuclear spin I and the rare earth spin S is of the form $A\mathbf{I} \cdot \mathbf{S}$, the Knight shift $K_f(T)$ can be written as

$$K_f(T) = -H_{\text{hf}} \langle S_z \rangle_{\text{av}} / H \quad (5)$$

where $H_{\text{hf}} = A/\gamma\hbar$ is the hyperfine field per unit spin, and γ is the gyromagnetic ratio of the resonant nucleus. For most of the rare earth ions, the thermal

average of the rare earth spin is related to the 4f susceptibility, i.e.

$$\langle S_z \rangle_{av}/H = -\chi_f(g_J - 1)/Ng_J\mu_B \quad (6)$$

where g_J is Lande's g -factor and N is the Avogadro number. Therefore, from equations 2, 4 and 5 we note that the Knight shift is linearly related to the susceptibility, and the corresponding equations become

$$K_f(T) = -K_0 \left[\frac{6\pi Z(g_J - 1)J(0)}{Ng_J\mu_B^2} \chi_f(T) \sum_n F(2k_f R_n) \right] \quad (7)$$

$$K_f(T) = K_0 J_{sf}(g_J - 1) \chi_f(T) / 2Ng_J\mu_B^2 \quad (8)$$

$$K_f(T) = (g_J - 1) H_{hf} \chi_f(T) / Ng_J\mu_B \quad (9)$$

Thus from the study of the Knight shift and the susceptibility one gets information regarding the magnitude and the sign of the exchange interaction constant J_{sf} or $J(0)$.

Although the RKKY theory is more realistic, there are certain assumptions which are not justified when it is applied to real metals. Moreover, interpretation in terms of the RKKY theory involves other unknown parameters. Therefore, throughout this paper we shall give either H_{hf} or J_{sf} values. It is obvious from equation 7 that $H_{hf} = K_0 J_{sf} / 2\mu_B = -6\pi Z J(0) K_0 / \mu_B \sum_n F(2k_f R_n)$ and we can go over from one model to another. However, this should not be taken to imply that the uniform polarization model is correct. In fact experiments have shown⁵⁻⁷ that the conduction electron polarization is not uniform.

In this paper we discuss the magnetic resonance studies in some cerium and samarium compounds in relation to their susceptibilities and other available data. Section II deals with cerium compounds and Section III with samarium compounds.

II. NUCLEAR MAGNETIC RESONANCE STUDIES IN SOME CERIUM COMPOUNDS IN RELATION TO THEIR MAGNETIC, ELECTRONIC AND TRANSPORT PROPERTIES

Cerium, both in pure elemental form and in several intermetallic compounds, exhibits peculiar magnetic, electronic and transport properties⁸. While many of the compounds containing cerium show behaviour characteristic of the trivalent cerium ion (electronic configuration $4f^1$), a few of the compounds exhibit Kondo-like phenomena. Yet there are a few other cerium compounds which fall into neither of the two categories mentioned above; $CeSn_3$ being one such compound. In this part of the paper we discuss magnetic resonance studies in $CePt_2$, $CePt_5$ and $CeSn_3$ in relation to their susceptibilities and other available data.

The intermetallic compound $CePt_2$ has the cubic C15 (Cu_2Mg type) structure. The local site symmetry at Ce sites is full cubic but is only axial at Pt sites. The magnetic susceptibility of $CePt_2$ has been measured by several workers⁵⁻⁹ and values of the effective paramagnetic moment $\mu_{eff} = 2.57 \pm 0.07^7$, 2.50^8 and $2.33\mu_B^9$ and the paramagnetic Curie temperature $\theta_p = -26^7$ and $5K^9$ have been reported. Joseph *et al.*⁹ find that $CePt_2$

orders antiferromagnetically with $T_N = 1.5$ to 1.7 K while van Daal and Buschow⁸ report it to be a ferromagnet with $T_C = 7$ K. Such a disparity between two different samples of CePt_2 might have arisen because of the fact that the C15 phase is known to extend¹⁰ right up to CePt_3 and it is likely that compounds with somewhat different homogeneity (and therefore having different magnetic behaviour) might be involved. The presence of a small amount of some other ferromagnetic phase of Ce–Pt in the sample also cannot be ruled out. Joseph *et al.*⁹ have explained their magnetic susceptibility and the heat capacity results of CePt_2 on the basis of Ce^{3+} ions perturbed by crystal fields. In the presence of a crystal field of cubic symmetry, the $J = \frac{5}{2}$ level of the Ce^{3+} ion splits into doublet and quartet energy levels. Such a splitting causes a reduction in the magnetic susceptibility compared to the free ion value, and also introduces a Schottky type of anomaly in the electronic specific heat. The experimental results are consistent with the crystal field split doublet ground state separated by 216 K from the quartet.

The ^{195}Pt Knight shift in CePt_2 has been measured^{5–7} from 300 to 113 K and is found to be proportional to the bulk susceptibility in the same temperature interval. The Knight shift values are 1.08 per cent at 295 K and 1.56 per cent at 113 K. The Knight shift K_0 (in the absence of s–f exchange interaction) has been measured in the isostructural LaPt_2 and is found to have a value of 0.69 per cent. From the plot of Knight shift versus the susceptibility with temperature as the implicit parameter (*Figure 1*), a value of -54 kOe is obtained for H_{hf} , which is close to the value obtained in other

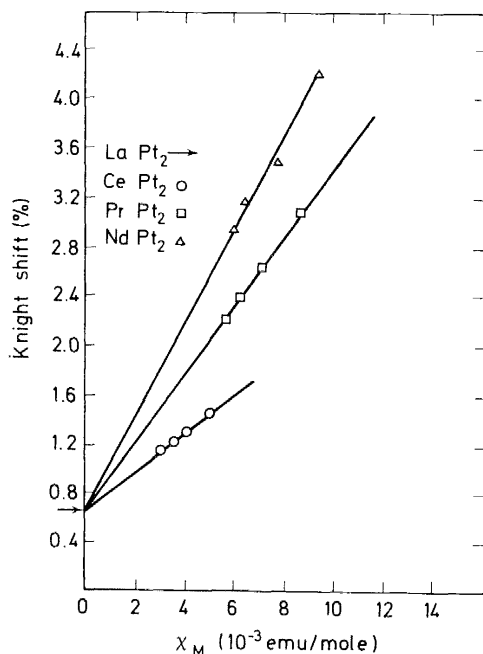


Figure 1. The ^{195}Pt Knight shift versus susceptibility (with temperature the implicit parameter) in CePt_2 , PrPt_2 and NdPt_2 .

RPt₂ compounds. The Knight shift measurements are being extended to low temperatures.

The compound CePt₅ has the hexagonal (CaCu₅ type) structure with two sets of platinum atoms arranged in alternate planes normal to the *c* axis. Those in the plane containing the rare earth atoms are designated as Pt_I and the others as Pt_{II} and they occur in the ratio of 2:3. Consequently two ¹⁹⁵Pt n.m.r. lines were observed with the relative intensity ratio of 2:3 and this enabled the lines to be assigned to the respective platinum sites. The ¹⁹⁵Pt Knight shifts at 295 K and 123 K are 1.22 per cent and 1.55 per cent for Pt_I and 0.36 per cent and 0.52 per cent for Pt_{II} sites^{5-7, 11}. The magnetic susceptibility of CePt₅ is close to that expected from Ce³⁺ ions perturbed by crystal fields^{5-7, 12}. The ¹⁹⁵Pt Knight shift at both the platinum sites is proportional to the bulk susceptibility. Figure 2 shows a plot of the Knight

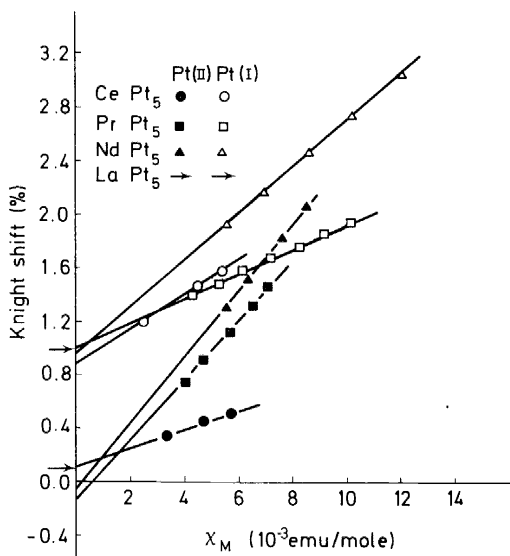


Figure 2. The ¹⁹⁵Pt Knight shift for the two Pt sites versus the susceptibility (with temperature the implicit parameter) in CePt₅, PrPt₅ and NdPt₅.

shift versus the susceptibility in CePt₅, PrPt₅ and NdPt₅, from which two interesting results are to be noted. Firstly, the Knight shift versus susceptibility curves have different slopes for Pt_I and Pt_{II} sites, and if interpreted in terms of the uniform polarization model, this would imply two different values of J_{sf} in one alloy, which is absurd. Secondly, the values of H_{hf} at the two Pt sites in CePt₅ do not correlate with the values in PrPt₅ and NdPt₅. For instance, while in CePt₅ we have $H_{hf}(Pt_I) = -44$ kOe and $H_{hf}(Pt_{II}) = -27$ kOe the corresponding values in PrPt₅ are -22.4 kOe and -45.6 kOe. In terms of the RKKY theory we note that $H_{hf}(Pt_I)/H_{hf}(Pt_{II}) = \Sigma Pt_I/\Sigma Pt_{II}$, where $\Sigma Pt_I(\Sigma Pt_{II})$ stands for $\Sigma_n F(2k_F R_n)$ with $Pt_I(Pt_{II})$ as the origin. Knight shift results in PrPt₅ and NdPt₅ imply that $\Sigma Pt_I < \Sigma Pt_{II}$. The RKKY sums ΣPt_I and ΣPt_{II} have been calculated and it is found that for a reasonable

choice of the Fermi wave vector k_F , we indeed have $H_{hf}(Pt_I)/H_{hf}(Pt_{II}) = \Sigma Pt_I/\Sigma Pt_{II}$ for $PrPt_5$ and $NdPt_5$. However, for the same choice of k_F the Knight shift results in $CePt_5$ are totally inconsistent with the RKKY sums. But if k_F is slightly increased (by about ten per cent) over the value in $PrPt_5$ and $NdPt_5$ then ΣPt_I becomes greater than ΣPt_{II} and the Knight shift results in $CePt_5$ can also be explained on the basis of RKKY theory. Keeping constant in all the alloys the number of electrons contributed by platinum to the conduction band, a small increase in k_F in $CePt_5$ can be obtained by assuming that cerium contributes slightly more than three electrons to the conduction band of the alloy. Thus the Knight shift results suggest either a valence of slightly more than three for cerium in $CePt_5$ or a breakdown of the RKKY theory. The Knight shift measurements in $CePt_5$ at low temperatures would throw more light on the nature of cerium ions.

The compound $CeSn_3$ has the f.c.c. $Cu_3Au(L1_2)$ type of crystal structure. The local symmetry at every cerium site is cubic. The magnetic susceptibility of $CeSn_3$ was originally measured by Tsuchida and Wallace¹³ in the temperature range of 2 to 300 K. Subsequently the temperature dependence of the susceptibility has been confirmed by the independent measurements of Shenoy *et al.*¹⁴, Ruggiero and Olcese¹⁵, Cooper *et al.*¹⁶ and Malik and Vijayaraghavan¹⁷. However, because of their limited temperature range Ruggiero and Olcese¹⁵ could observe only the beginning of the anomalous low temperature behaviour of susceptibility of $CeSn_3$, while the low temperature results of Cooper *et al.*¹⁶ are not very accurate. The temperature dependence of the susceptibility is shown in *Figure 3* and it has the following salient features. Above about 250 K the susceptibility seems to follow a Curie-

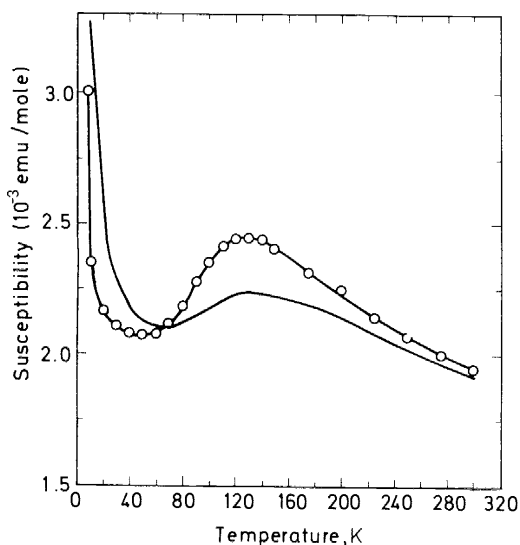


Figure 3. Magnetic susceptibility χ of $CeSn_3$ versus the temperature. The curve with experimental points is from the unpublished results of Malik and Vijayaraghavan while the smooth curve has been obtained from $1/\chi$ values given by Tsuchida and Wallace¹³.

Weiss law with an unusually large value of the paramagnetic Curie temperature. The temperature range over which the Curie-Weiss law is obeyed is too small to obtain any meaningful value of the paramagnetic moment. Around 135 K there is a broad maximum in the susceptibility followed by a rapid rise below 30 K. The measurements of Malik and Vijayaraghavan (also shown in *Figure 3*) show a less rapid rise than that observed by Tsuchida and Wallace¹³. At low temperatures the susceptibility is much less than that expected on the basis of trivalent cerium ions. Crystal field effects alone cannot explain the peculiar susceptibility behaviour of CeSn_3 . As mentioned in connection with the susceptibility of CePt_2 , the crystal fields, in general, tend to reduce the susceptibility from the free ion value.

Tsuchida and Wallace¹³ suggested that the broad maximum in the susceptibility of CeSn_3 might arise from a partial conversion of magnetic Ce^{3+} ($4f^1$) ions to non-magnetic Ce^{4+} ($4f^0$) ions. From the temperature dependence of the lattice constant, Harris and Raynor¹⁸ concluded that the valence of cerium in CeSn_3 was close to 3.1. The Sn Mössbauer results of Kanekar *et al.*¹⁹ supported the $\text{Ce}^{3+} \rightarrow \text{Ce}^{4+}$ conversion. However, subsequent Mössbauer studies by Shenoy *et al.*¹⁴ in the temperature range of 1.6 to 293 K revealed no change either in the isomer shift or in the electric field gradient on Sn over the temperature range in which the valence change was presumed to be occurring. The rapid rise in the susceptibility below 30 K was attributed by Tsuchida and Wallace¹³ to the onset of incipient ferromagnetism. The Sn n.m.r. in CeSn_3 has been studied in the temperature range 300 K to 77 K by Rao and Vijayaraghavan²⁰ and by Borsa *et al.*²¹. The n.m.r. measurements were extended up to 1.2 K by Malik *et al.*²² and the observation of the Sn n.m.r. line down to 1.2 K suggests that CeSn_3 does not order ferromagnetically up to this temperature. Moreover, the Sn Knight shift was found not to follow the bulk susceptibility.

Detailed studies of the Knight shift and the spin lattice relaxation time of ^{119}Sn in CeSn_3 have been carried out recently by the present authors. The ^{119}Sn n.m.r. experiments were performed using a Bruker B-KR 323s pulsed n.m.r. spectrometer operating at a frequency of 16 MHz. A Bruker B-E 38 electromagnet provided the polarizing magnetic field and a Hall-effect device regulated and swept the magnetic field. The method used for observing the n.m.r. is that suggested by Clark²³. The external field is swept through the ^{119}Sn signal and the entire free induction decay (FID) signal is processed by a 'boxcar' integrator using a time constant much greater than the FID length. The output of the boxcar then provided a reproduction of the absorption spectrum over the range of field swept. Time averaging in order to improve the signal to noise ratio was effected by means of a Digital Equipment Corporation PDP-8L computer. Temperature variation was achieved using a liquid helium cryostat equipped with an elongated tailpiece to fit in the magnet gap. The temperature was controlled using a Varian variable temperature controller, or a home built unit, with either platinum or carbon resistors as sensing elements. Temperatures were measured using a copper-constantan thermocouple, or a germanium resistor thermometer (< 70 K). The ^{119}Sn Knight shift is plotted in *Figure 4* as a function of temperature along with the magnetic susceptibility results of Malik and Vijayaraghavan. It is to be noted that although the ^{119}Sn Knight shift also shows a broad

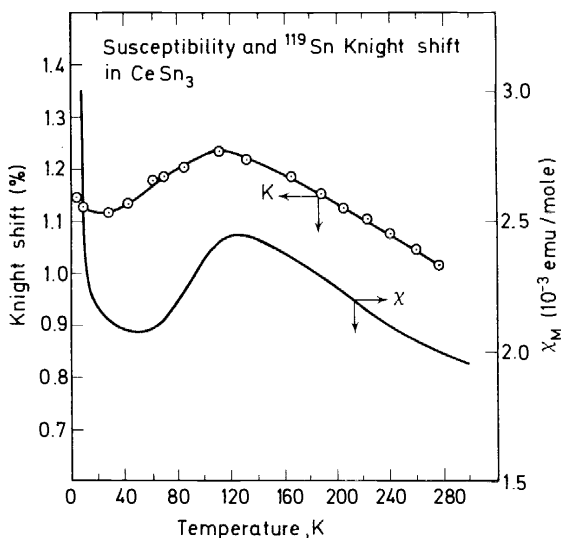


Figure 4. The ^{119}Sn Knight shift in CeSn_3 versus temperature (present work) and magnetic susceptibility of CeSn_3 versus temperature (Malik and Vijayaraghavan).

maximum around 115 K, the linear relationship between the Knight shift and the bulk susceptibility is lacking; in particular, unlike the susceptibility, the ^{119}Sn Knight shift does not show a rapid rise below 30 K. The spin lattice relaxation time T_1 of Sn in CeSn_3 has also been measured at various temperatures and is shown in Figure 5. At low temperature $T_1 T$ approaches the value in pure Sn metal. The ^{119}Sn Knight shift and T_1 in $\text{CeSn}_x\text{In}_{3-x}$ have

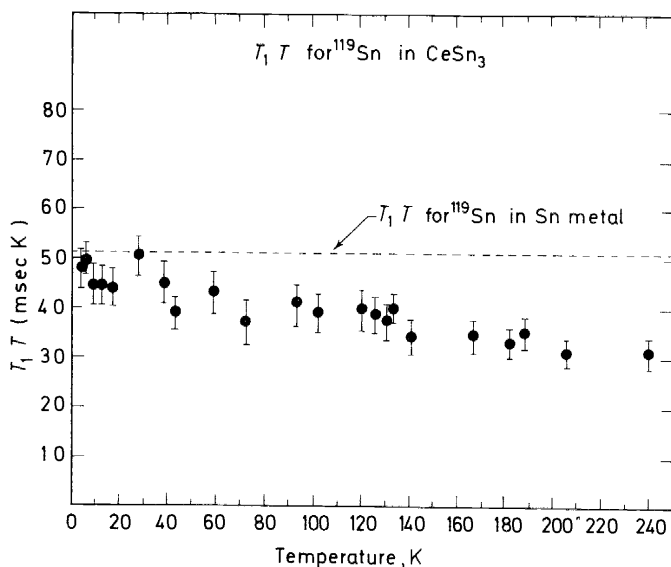


Figure 5. The ^{119}Sn spin-lattice relaxation time $T_1 T$ in CeSn_3 versus the temperature (T).

been studied by Welsh and Darby²⁴ for $0.6 \leq x \leq 3.0$, from which they conclude that the n.m.r. results in CeSn_3 are consistent with Ce f-electrons occupying a virtual bound state and as In is substituted for Sn the Ce f-electrons become more and more localized. Myers and Narath²⁵ also find that in CeP and CeAs, the ^{31}P and ^{75}As Knight shifts do not follow the respective bulk susceptibilities. The absence of a correlation between the Knight shift and the bulk susceptibility in CeSn_3 , CeP and CeAs suggests that either the electronic structure of cerium in these compounds is very different from that of Ce^{3+} (so that the RKKY theory is not valid) or the electron nuclear interaction is anisotropic.

The electrical resistivity of polycrystalline CeSn_3 has been measured by Cooper *et al.*¹⁶ and of single crystal CeSn_3 by Stalinski *et al.*²⁶. The results of the measurement of electrical resistance of three different samples of CeSn_3 by Cooper *et al.*¹⁶ are shown in Figure 6. The resistivity does not show a Kondo-type minimum. On the other hand, at low temperatures ($T \lesssim 17$ K) the resistivity follows T^2 law which is expected²⁷ in the presence of paramagnons or localized spin fluctuations^{28,29}. The electronic specific heat of CeSn_3 shows an upturn (increase with decreasing temperature) below $T^2 \simeq 10 \text{ K}^2$ (Figure 7) and the coefficient γ of the electronic specific heat ($C = \gamma T$) is very large ($\gamma \simeq 53 \text{ mJ/mol K}^2$)¹⁶. A similar behaviour has also been observed³⁰ in the case of CeNi_2 . The upturn in specific heat cannot be attributed to hyperfine interaction since various stable isotopes of cerium lack both magnetic and the quadrupole moments. The large γ value in CeSn_3 implies a sizeable 4f occupation near the Fermi level even though the state is non-magnetic. The thermoelectric power of CeSn_3 has been measured by Cooper *et al.*¹⁶ and shows a broad maximum.

The anomalous behaviour of cerium in pure metal form or in intermetallic compounds is usually attributed to the proximity of the 4f level of cerium

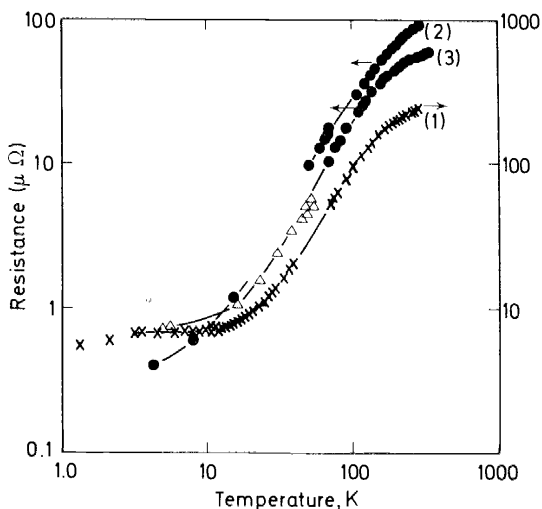


Figure 6. Resistance versus temperature (log-log scale) for three different samples of CeSn_3 . Sample number 3 was used for n.m.r. and susceptibility measurements.

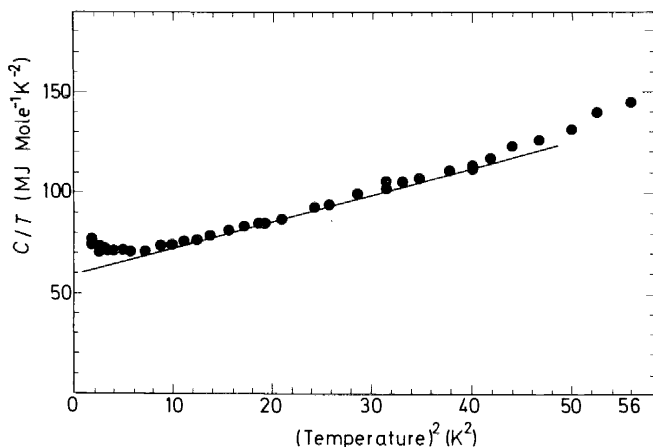


Figure 7. Specific heat C/T versus temperature² in CeSn_3 .

to the Fermi level³¹. Thus the change in lattice constant is supposed to arise due to a promotion of the 4f electron to the conduction band. Similarly, the hybridization between the 4f electron states and the conduction band is responsible for the Kondo behaviour³². Behaviour characteristic of trivalent cerium is observed only if the 4f levels lie very much below the Fermi level (E_F). The large γ value in CeSn_3 implies a sizeable 4f occupation near E_F . Therefore the susceptibility behaviour of CeSn_3 might arise due to the movement of the 4f level relative to the Fermi level as a function of temperature³¹. When the 4f level lies above E_F the system becomes non-magnetic. This appears as a transformation from magnetic (Ce^{3+}) to non-magnetic (Ce^{4+}) ions. Though this may explain the small value of the susceptibility of CeSn_3 at low temperatures, the broad peak in the susceptibility and the rapid rise below 30 K cannot be understood in this manner. Moreover, when the 4f level is close to E_F , phenomena like spin fluctuations²⁷⁻²⁹ also become important. The spin fluctuations or the paramagnons enhance the susceptibility and the γ value and give rise to a T^2 term in the resistivity, the latter having been observed²⁶ recently with CeSn_3 . However, in the presence of spin fluctuations the susceptibility should level off (or reach a constant value) at low temperatures, which does not happen. It may also be mentioned that all the rise in susceptibility below 30 K may not be genuine since Malik and Vijayaraghavan have observed a less rapid rise than that observed by Tsuchida and Wallace (Figure 3). Kondo effect in the presence of crystal fields may also lead to an abnormal temperature dependence of the susceptibility³³. Recently, Misawa³⁴ has analysed the susceptibility of CeSn_3 following the Fermi liquid model and has attributed the broad peak at about 150 K to the $T^2 \ln T$ dependence of the susceptibility inherent in this model. It would be interesting to see what happens to the Knight shift of the non-magnetic site in the Fermi liquid model.

In conclusion we note that the magnetic behaviour of CePt_2 and to some extent that of CePt_5 can be adequately explained on the basis of Ce^{3+}

ions perturbed by crystal fields. The compound CeSn_3 behaves in an anomalous fashion. Though the large γ value and the broad peak in susceptibility can be understood following the Fermi liquid model, there is no adequate explanation for many other experimentally observed results such as the rapid rise in susceptibility below 30 K, the absence of the correlation between the Knight shift and the susceptibility, the upturn in the specific heat etc.

III. MAGNETIC RESONANCE STUDIES IN SAMARIUM COMPOUNDS

Introduction

Alloys and compounds containing samarium are known to exhibit peculiar magnetic properties. In order to understand the magnetism of samarium let us look more closely at the electronic structure and energy levels of the Sm^{3+} ion. The Sm^{3+} ion possesses five electrons in the 4f shell which are responsible for its magnetic and spectroscopic properties. The lowest spectroscopic term given by the Hund's rule is 6H ($S = 5/2$ and $L = 5$, where S is the spin angular momentum quantum number and L is the orbital angular momentum quantum number). This term is split by the spin-orbit interaction into a number of levels each characterized by a definite value of J the total angular momentum. These levels form components of an LS multiplet, and the quantum number J can assume the range of values $J = (L - S), (L - S + 1) \dots (L + S - 1), (L + S)$, i.e. $J = \frac{5}{2}, \frac{7}{2}, \dots, \frac{15}{2}$ with $J = \frac{5}{2}$ as the ground level. Unlike in most other rare earth ions, the multiplet width in the case of Sm^{3+} ion is very small; the energy separation between the ground ($J = \frac{5}{2}$) level and the first excited ($J = \frac{7}{2}$) level is only about 1 400 to 1 500 K. As a result of the narrow multiplet width, temperature independent Van Vleck terms, associated with the second-order Zeeman effect, contribute appreciably to various observable quantities concerning the Sm^{3+} ion, such as the susceptibility χ_f due to 4f electrons³⁵, the thermal average of the Sm^{3+} spin³⁶, the 4f-induced hyperfine field at the samarium nuclear site³⁷ etc.

As mentioned earlier, in rare earth intermetallic compounds, the 4f contribution to the Knight shift (K_f) of the non-magnetic site is proportional to the thermal average ($\langle S_z \rangle_{\text{av}}/H$) of the rare earth spin. In rare earth ions where only the ground multiplet level is mainly populated (to be called the 'normal' rare earth ions), $\langle S_z \rangle_{\text{av}}/H$ is proportional to χ_f so that a linear relation exists between K_f and χ_f . However, with the Sm^{3+} ion, because of the temperature independent contributions, the linear relation between K_f and χ_f is no longer valid³⁶. Further, White and Van Vleck³⁶ showed that in samarium compounds, where Sm^{3+} ions could be considered as 'free' ions, $\langle S_z \rangle_{\text{av}}/H$ shows a crossover, i.e. passes through zero, at a temperature of about 300 K, called the crossover temperature (T_{co}). The crossover in $\langle S_z \rangle_{\text{av}}/H$ at the expected temperature has, indeed, been observed in SmX ($X = \text{P}, \text{As}, \text{Sb}, \text{Bi}$)^{38, 39} and SmAl_3 ⁴⁰ by studying the 4f contribution to the Knight shift of the non-magnetic site. However, Knight shift measurements in some other samarium compounds showed that the crossover may occur at a temperature lower than 300 K, e.g. $T_{\text{co}} = 230 \pm 20$ K in SmPt_2 ⁴¹, or the crossover may be completely absent as in SmAl_2 ⁴², SmSn_3 ^{20, 2f, 41, 43} and

SmF_3 ⁴⁴. White and Van Vleck³⁶ had suggested that the splitting of the ground ($J = \frac{5}{2}$) state by cubic crystal fields may reduce the crossover temperature (T_{co}) from 300 K. However, the reduction in T_{co} , even for sizeable crystal field splittings, is not appreciable. It was then shown by Malik and Vijayaraghavan^{45,46} and by Malik⁷ that the anomalous behaviour of the Knight shift in samarium compounds arises as a result of the mixing of the excited ($J = \frac{7}{2}$) multiplet level into the ground ($J = \frac{5}{2}$) level by crystal fields.

In this part of the paper, we discuss the effects of cubic crystal fields and the exchange interaction on various observable quantities concerning the Sm^{3+} ion, such as the susceptibility due to 4f electrons, the thermal average of the 4f spin, the 4f induced hyperfine field at the samarium nuclear site in the paramagnetic and ferromagnetic states, the saturation magnetic moment and the temperature dependence of Sm^{3+} magnetization, etc. The crystal field Hamiltonian is introduced and its matrix elements between states in the (SLJM) representation including those non-diagonal in J are obtained. The calculations are performed taking into account the admixture of excited J levels into the ground level of Sm^{3+} by crystal fields and exchange fields. It is shown that the crystal fields may reduce the crossover temperature in $\langle S_z \rangle_{av}/H$ from 300 K to lower values or even completely suppress the crossover. In some cases the crystal fields may give rise to more than one crossover in $\langle S_z \rangle_{av}/H$. On the other hand, although the 4f-induced hyperfine field H_{4f}/H on the samarium nucleus in the paramagnetic state is positive in the case of free Sm^{3+} ion, the crystal fields bring about one or more crossovers in H_{4f}/H . In the ferromagnetic state also the crystal fields may make H_{4f} negative from its positive value in the free Sm^{3+} ion. Moreover, the crystal fields may reduce or even enhance the magnetic moment of the Sm^{3+} ion and force it to behave effectively like an ($L + S$) ion rather than an ($L - S$) ion. The samarium magnetization also shows a crossover, the temperature of which depends upon the crystal fields.

The crystal field Hamiltonian and its matrix elements

The general crystal field Hamiltonian may be written as⁴⁷

$$\mathcal{H}_C = \sum_{n=0}^{\infty} \sum_{m=0}^n A_n^m \sum_i f_{nm}^c(\mathbf{r}_i) \quad (10)$$

where the $f_{nm}^c(\mathbf{r})$, which have been tabulated by Hutchings⁴⁷, are certain functions of the Cartesian coordinates of the electrons. The summation involving i is over all the electrons of the partially filled shell, the 4f-shell in our case. The first term in equation 10 corresponding to $n = m = 0$ is a constant which, in the first approximation, gives a uniform shift in energy of all the levels of a configuration and may be ignored as far as the crystal field splitting of the levels is concerned. All the terms with n -odd vanish in equation 10 for configurations containing solely equivalent electrons (electrons possessing same n and l quantum numbers). This is because parity is a good quantum number within a given configuration. For f ($l = 3$) electrons, only terms with $n \leq 6$ give non-zero contributions. Further, the point symmetry of the ion under consideration may require that some of the terms in equation 10 be

zero. For ions located at points of very high symmetry the coefficients with the same n may be related (as is found in the cubic case).

While working in a manifold of states corresponding to a single value of J , it is convenient to use the method of operator equivalents. In this method one replaces $f_{nm}^c(\mathbf{r})$ by the angular momentum operators, i.e.

$$A_n^m \sum_i f_{nm}^c(\mathbf{r}_i) = [A_n^m \langle r^n \rangle \theta_n] O_n^m = B_n^m O_n^m \quad (11)$$

where $\theta_n = \alpha, \beta, \gamma$ are the operator equivalent factors for the second, the fourth and the sixth degree terms in the crystal potential. The O_n^m are certain polynomials involving angular momentum operators and act on the angular part of the wave function. The radial integration is assumed to have been carried out and $\langle r^n \rangle$ is the expectation value of the n th power of the radius of the 4f orbital. The factors θ_n for different rare earth ions and the operators O_n^m have been tabulated by Hutchings^{4,7}. For calculations involving the crystal field effects on the Sm^{3+} ion, we need matrix elements of the crystal field Hamiltonian between states belonging to different J manifolds. These can also be obtained by the method of operator equivalents extended to elements non-diagonal in J ^{4,8-51}. However, it is convenient to use the tensor operator techniques to obtain these matrix elements. The crystal field Hamiltonian is written in terms of the tensor operators $C_m^{(n)}$ by making the following replacements

$$f_{n0}^c(\mathbf{r}) = a_{n0} r^n C_0^{(n)}(\theta, \phi) \quad (12a)$$

$$f_{nm}^c(\mathbf{r}) = a_{nm} r^n [C_{-m}^{(n)}(\theta, \phi) + (-1)^m C_m^{(n)}(\theta, \phi)]_{m>0} \quad (12b)$$

where $C_m^{(n)}(\theta, \phi)$ are defined in terms of the spherical harmonics as

$$C_m^{(n)}(\theta, \phi) = [4\pi/(2n+1)]^{\frac{1}{2}} Y_n^m(\theta, \phi) \quad (13)$$

and a_{nm} are certain numerical factors which can be easily determined by comparing the two sides of equations 12a and 12b, for example $a_{40} = 8$ and $a_{60} = 16$. The radial integration over the 4f wave function may be carried out on the RHS of equations 12a and 12b to obtain $\langle r^n \rangle$. The operators $C_m^{(n)}$ act only on the angular part of the wave function and we need their matrix elements between different states in the ($f^N \alpha$ SLJM) representation. (Here α stands for a set of any other quantum numbers necessary to specify the state.) The matrix elements of $C_m^{(n)}$ are diagonal in the spin variables. The M dependence of the matrix elements can be taken apart by the Wigner-Eckart theorem, i.e.

$$(f^N \alpha \text{SLJM} | C_m^{(n)} | f^N \alpha' \text{SL}'J'M') = (-1)^{J-M} \begin{pmatrix} J & n & J' \\ -M & m & M' \end{pmatrix} \times (f^N \alpha \text{SLJ} \| C^{(n)} \| f^N \alpha' \text{SL}'J') \quad (14)$$

where the large parenthesis denotes the Wigner 3- j symbol. The reduced matrix elements of $C^{(n)}$ can be written as⁵²

$$(f^N \alpha \text{SLJ} \| C^{(n)} \| f^N \alpha' \text{SL}'J') = (-1)^{S+L'+J+n} [(2J+1)(2J'+1)]^{\frac{1}{2}} (f \| C^{(n)} \| f) \times \begin{Bmatrix} J & J' & n \\ L & L & S \end{Bmatrix} (f^N \alpha \text{SL} \| U^{(n)} \| f^N \alpha' \text{SL}) \quad (15)$$

where

$$(f \| C^{(n)} \| f) = (-1)^l (2l + 1) \begin{pmatrix} l & n & l \\ 0 & 0 & 0 \end{pmatrix} \quad (16)$$

and $l = 3$ for f electrons. The curly parenthesis in equation 15 denotes the Wigner $6-j$ symbol. The $3-j$ and $6-j$ symbols have been tabulated by Rotenberg *et al.*⁵³. The doubly reduced matrix elements of the unit tensor operator $U^{(n)}$ for various rare earth ion configurations have been tabulated by Nielson and Koster⁵⁴ and can be obtained⁵² by making use of the coefficients of fractional parentage. For the ${}^6H(S = \frac{5}{2}, L = 5)$ multiplet of Sm^{3+} the values of $(SL \| U^{(n)} \| SL)$ are

$$\left(\frac{5}{2}, 5 \| U^{(2)} \| \frac{5}{2}, 5\right) = -\frac{1}{3} [(11 \times 13)/(2 \times 7)]^{\frac{1}{2}}$$

$$\left(\frac{5}{2}, 5 \| U^{(4)} \| \frac{5}{2}, 5\right) = \frac{2}{3} [13/7]^{\frac{1}{2}}$$

$$\left(\frac{5}{2}, 5 \| U^{(6)} \| \frac{5}{2}, 5\right) = +\frac{1}{3} [5 \times 17/7]^{\frac{1}{2}}$$

Thus by making use of the reduced matrix elements of $U^{(n)}$ and equations 14 to 16, all the required matrix elements of the crystal field Hamiltonian can be completely determined.

In this paper we shall confine our attention to cubic samarium compounds in which Sm^{3+} ions occupy a site of local cubic symmetry. The cubic crystal field Hamiltonian for the choice of the quantization axis (z axis) parallel to $[001]$ is given by⁴⁷

$$\mathcal{H}_C = A_4^0 \sum_i [f_{40}^c(\mathbf{r}_i) + 5f_{44}^c(\mathbf{r}_i)] + A_6^0 \sum_i [f_{60}^c(\mathbf{r}_i) - 21f_{64}^c(\mathbf{r}_i)] \quad (17)$$

where we have made use of the fact that for $z \parallel [001]$, some of the coefficients A_m^n are related, namely $A_4^4 = 5A_4^0$ and $A_6^6 = -21A_6^0$. We shall abbreviate A_4^0 to A_4 and A_6^0 to A_6 . In terms of the tensor operators $C_m^{(n)}$ the cubic crystal field Hamiltonian can be written as

$$\begin{aligned} \mathcal{H}_C = 8A_4 \langle r^4 \rangle \sum \left[C_0^{(4)} + \left(\frac{5}{14}\right)^{\frac{1}{2}} (C_{-4}^{(4)} + C_4^{(4)}) \right] \\ + 16A_6 \langle r^6 \rangle \sum \left[C_0^{(6)} - \left(\frac{7}{2}\right)^{\frac{1}{2}} (C_{-4}^{(6)} + C_4^{(6)}) \right] \end{aligned} \quad (18)$$

(We drop the arguments of $C_m^{(n)}$ as well as the summation index for the sake of brevity.) The coefficients $A_4 \langle r^4 \rangle$ and $A_6 \langle r^6 \rangle$ determine the strength of the fourth and the sixth degree terms, respectively, in the crystal field Hamiltonian. We shall treat them as parameters in our calculations to show the kinds of effects to be expected as the magnitude of one over the other is varied.

Calculation of susceptibility and spin average

We assume that Russell-Saunders coupling holds and multiplet levels conform to the cosine law $\mathcal{H}_0 = \lambda \mathbf{L} \cdot \mathbf{S}$. The energy of each multiplet level is given by

$$E_J = \frac{1}{2} \lambda [J(J + 1) - L(L + 1) - S(S + 1)] \quad (19)$$

We shall now calculate the $4f$ -electron susceptibility and the spin average. While calculating these quantities for Sm^{3+} ions in the presence of an

externally applied magnetic field H , which acts on $(L_z + 2S_z)$, and an exchange field H_{ex} , which acts on S_z , we note that both $(L_z + 2S_z)$ and S_z have matrix elements non-diagonal in J . This is because \mathbf{S} and $\mathbf{L} + 2\mathbf{S}$, unlike $\mathbf{J} = \mathbf{L} + \mathbf{S}$, are not constants of the motion. Consequently, the applied and the exchange fields admix different J states. Both \mathbf{L} and \mathbf{S} , being vectors, connect states differing in J by 0 or ± 1 . The non-vanishing matrix elements of the z-components of the spin and the orbital angular momentum operators between states given in the (SLJM) representation are:

$$\langle \text{SLJM} | S_z | \text{SLJM} \rangle = (g_J - 1)M \quad (20a)$$

$$\langle \text{SLJM} | L_z + 2S_z | \text{SLJM} \rangle = g_J M \quad (20b)$$

$$\langle \text{SLJM} | S_z | \text{SLJ} + 1M \rangle = \langle \text{SLJ} + 1M | S_z | \text{SLJM} \rangle = [(J + 1)^2 - M^2]^{\frac{1}{2}} \times \langle J || \Delta || J + 1 \rangle \quad (20c)$$

Since $L_z + S_z = J_z$ is diagonal in its own representation we have

$$\begin{aligned} \langle \text{SLJM} | L_z | \text{SLJ} + 1M \rangle &= \langle \text{SLJ} + 1M | L_z | \text{SLJM} \rangle \\ &= -[(J + 1)^2 - M^2]^{\frac{1}{2}} \langle J || \Delta || J + 1 \rangle \end{aligned} \quad (20d)$$

so that

$$\begin{aligned} \langle \text{SLJM} | L_z + 2S_z | \text{SLJ} + 1M \rangle &= \langle \text{SLJ} + 1M | L_z + 2S_z | \text{SLJM} \rangle \\ &= [(J + 1)^2 - M^2]^{\frac{1}{2}} \langle J || \Delta || J + 1 \rangle \end{aligned} \quad (20e)$$

where g_J is the Lande g factor and the multiplicative factor $\langle J || \Delta || J + 1 \rangle$ is given by

$$\begin{aligned} &\langle J || \Delta || J + 1 \rangle \\ &= \left[\frac{(J + L + S + 2)(-J + S + L)(J + L - S + 1)(J + S - L + 1)}{4(J + 1)^2(2J + 1)(2J + 3)} \right]^{\frac{1}{2}} \end{aligned} \quad (21)$$

The matrix elements of the form $\langle \text{SLJ} - 1M | S_z | \text{SLJM} \rangle$ etc. can be easily obtained from the expressions given above by lowering J by one unit.

The calculation of susceptibility and the spin average proceeds as follows. The Hamiltonian consisting of the spin-orbit coupling, the crystal field and the Zeeman term, i.e.

$$\mathcal{H} = \lambda \mathbf{L} \cdot \mathbf{S} + \mathcal{H}_C + \mu_B H (L_z + 2S_z) \quad (22)$$

is diagonalized within the substates arising from the lowest three multiplet levels ($J = \frac{5}{2}$, $J = \frac{7}{2}$ and $J = \frac{9}{2}$) to obtain the energy eigenvalues $E_m^{(0)}$ and the eigenfunctions $|m\rangle$. Neglecting $J = \frac{11}{2}$ and other higher levels reduces the size of the matrix to be diagonalized without at the same time introducing any significant errors, because these levels lie far off in energy. The susceptibility and the spin average are respectively given by

$$\chi_f = -N\mu_B \langle L_z + 2S_z \rangle_{\text{av}} / H = (-N\mu_B / H) \sum_m \langle m | L_z + 2S_z | m \rangle p(m) \quad (23)$$

and

$$\langle S_z \rangle_{\text{av}} / H = (1/H) \sum_m \langle m | S_z | m \rangle p(m) \quad (24)$$

where

$$p(m) = \exp(-E_m^{(0)}/kT) / \sum_m \exp(-E_m^{(0)}/kT) \quad (25)$$

is the Boltzmann factor for the state $|m\rangle$. In an alternative procedure⁵⁵ instead of diagonalizing the Hamiltonian of equation 22, one may diagonalize $\mathcal{H}' = \lambda \mathbf{L} \cdot \mathbf{S} + \mathcal{H}_C$ and treat the Zeeman term $\mu_B H(L_z + 2S_z)$ as a perturbation over the energy eigenvalues and the eigenfunctions obtained after diagonalizing \mathcal{H}' . We find that these two methods lead to identical results.

The results of the numerical calculations of $\langle S_z \rangle_{av}/H$ and χ_f as a function of temperature for various combinations of crystal field parameters $A_4\langle r^4 \rangle$ and $A_6\langle r^6 \rangle$ are shown in *Figure 8* and *Figure 9*. In all the calculations the spin-orbit coupling parameter has been taken to be $\lambda/k = 410$ K which gives an energy separation of 1435 K between the ground ($J = \frac{5}{2}$) level and the first excited ($J = \frac{7}{2}$) level. In *Figure 8* the temperature dependence of $\langle S_z \rangle_{av}/H$ is shown and the curves are labelled with the values of $A_4\langle r^4 \rangle/k$ and $A_6\langle r^6 \rangle/k$ in Kelvin. In the case of the free Sm^{3+} ion $\langle S_z \rangle_{av}/H$ shows a crossover at 300 K (curve marked free ion). However, as the strength of the crystal field is increased, either by changing $A_4\langle r^4 \rangle$ with $A_6\langle r^6 \rangle$ constant (solid curves) or by changing $A_6\langle r^6 \rangle$ with $A_4\langle r^4 \rangle$ constant (dotted curves), the crossover temperature decreases and eventually for sufficiently strong crystal fields the crossover completely disappears and $\langle S_z \rangle_{av}/H$ becomes negative

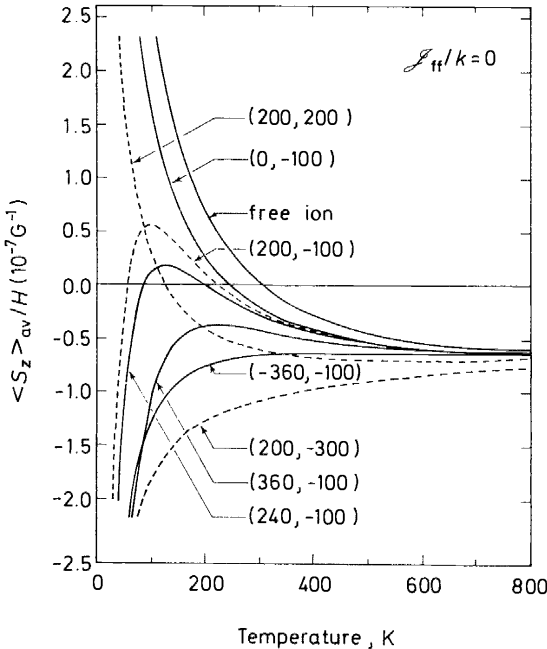


Figure 8. Effect of variation of $A_6\langle r^6 \rangle$ (solid curves) and $A_4\langle r^4 \rangle$ (dotted curves) on $\langle S_z \rangle_{av}/H$ of Sm^{3+} ion in a cubic crystal field. The numbers in parentheses are respectively the values of $A_4\langle r^4 \rangle/k$ and $A_6\langle r^6 \rangle/k$ in Kelvin.

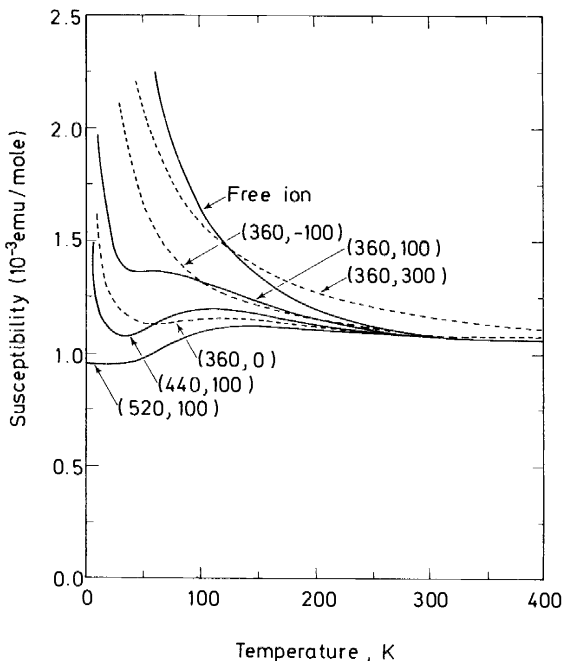


Figure 9. Effect of variation of $A_6\langle r^6 \rangle$ (solid curves) and $A_4\langle r^4 \rangle$ (dotted curves) on the susceptibility of Sm^{3+} ion in a cubic crystal field. The numbers in parentheses are respectively the values of $A_4\langle r^4 \rangle/k$ and $A_6\langle r^6 \rangle/k$ in Kelvin.

throughout. For some combinations of crystal field parameters more than one crossover occurs though such a behaviour has not been experimentally observed so far. Thus we see that the crystal fields strongly influence the crossover temperatures as well as the magnitude of $\langle S_z \rangle_{\text{av}}/H$. In Figure 9 the temperature dependence of the susceptibility is shown. At low temperatures the crystal fields reduce the susceptibility from the free ion value, and for some combinations of the crystal field parameters a hump appears in the χ_f versus T curve and the susceptibility decreases with decreasing temperatures.

Effect of exchange in the presence of crystal fields

The effect of exchange interaction between samarium ions can be treated as a perturbation over the eigenfunction and the eigenvalues obtained after diagonalizing the Hamiltonian given by equation 22. The perturbation Hamiltonian is

$$\mathcal{H}_{\text{pert}} = 2\mu_B H_{\text{ex}} S_z \quad (26)$$

(Again, one may use both Zeeman and exchange terms as perturbations on \mathcal{H}'). We calculate up to second order in perturbation theory the expectation values $\langle S_z \rangle$ and $\langle L_z + 2S_z \rangle$ of each level. Performing Boltzmann averaging of the expectation values over all the $|m\rangle$ sublevels and retaining terms linear in H_{ex} , we get

$$\langle S_z \rangle_{\text{av}} = \langle S_z \rangle_{\text{av}}^0 + 2\mu_B H_{\text{ex}} \sigma_{S,S} \quad (27)$$

and

$$\langle L_z + 2S_z \rangle_{\text{av}} = \langle L_z + 2S_z \rangle_{\text{av}}^0 + 2\mu H_{\text{ex}} \sigma_{L+2S,S} \quad (28)$$

where $\langle S_z \rangle_{\text{av}}^0$ denotes the Boltzmann average of the expectation value of S_z in the absence of exchange interactions, and likewise $\langle L_z + 2S_z \rangle_{\text{av}}^0$ denotes the corresponding quantity in the absence of exchange. The abbreviation $\sigma_{A,B}$ stands for⁵⁵

$$\sigma_{A,B} = \sigma_{B,A} = \sum_m \left[-\frac{\langle m|A_z|m\rangle \langle m|B_z|m\rangle}{kT} + 2 \sum_{m' \neq m} \frac{\langle m|A_z|m'\rangle \langle m'|B_z|m\rangle}{E_m^{(0)} - E_{m'}^{(0)}} \right] p(m) \quad (29)$$

with $p(m)$ given by equation 25. We use the molecular field approximation, in which the exchange field is given by

$$2\mu_B H_{\text{ex}} = -\mathcal{J}_{\text{ff}} \langle S_z \rangle_{\text{av}} \quad (30)$$

Substituting for H_{ex} and rearranging, we get

$$\frac{\langle S_z \rangle_{\text{av}}}{H} = \frac{\langle S_z \rangle_{\text{av}}^0}{H} [1 + \mathcal{J}_{\text{ff}} \sigma_{S,S}]^{-1} \quad (31)$$

and

$$\frac{\langle L_z + 2S_z \rangle_{\text{av}}}{H} = \frac{\langle L_z + 2S_z \rangle_{\text{av}}^0}{H} - \mathcal{J}_{\text{ff}} \sigma_{L+2S,S} \frac{\langle S_z \rangle_{\text{av}}^0}{H} [1 + \mathcal{J}_{\text{ff}} \sigma_{S,S}]^{-1} \quad (32)$$

Equation 31 brings out an interesting result, namely, $\langle S_z \rangle_{\text{av}}/H$ in the presence of exchange interaction is proportional to the corresponding value in the absence of exchange interaction. Thus, if in the absence of exchange interaction there is a crossover in $\langle S_z \rangle_{\text{av}}/H$ (i.e. it passes through zero), the crossover temperature T_{co} is not altered by the presence of exchange interaction, provided of course that T_{co} is higher than the temperature θ_f where $\langle S_z \rangle_{\text{av}}/H$ diverges. If T_{co} lies lower than θ_f , it would appear as if the exchange interaction has modified T_{co} , while actually the system is no longer paramagnetic.

The effect of exchange interaction on $\langle S_z \rangle_{\text{av}}/H$ is shown in *Figure 10* for an arbitrary set of crystal field parameters. The curves are labelled with the values of $\mathcal{J}_{\text{ff}}/k$ in Kelvin. It is to be noted that the introduction of the exchange interaction modifies the magnitude of $\langle S_z \rangle_{\text{av}}$ but not T_{co} so long as $T_{\text{co}} > \theta_f$. However, when \mathcal{J}_{ff} is increased sufficiently the system orders magnetically even before T_{co} is reached and one gets the impression as if the exchange interaction has suppressed the crossover temperature. The effect of exchange interaction on the susceptibility is shown in *Figure 11*. A ferromagnetic exchange interaction (positive \mathcal{J}_{ff}) increases the magnitude of χ_f and $\langle S_z \rangle_{\text{av}}/H$ compared to the values in the absence of exchange interaction, while an

STUDIES ON SOME CE AND SM COMPOUNDS

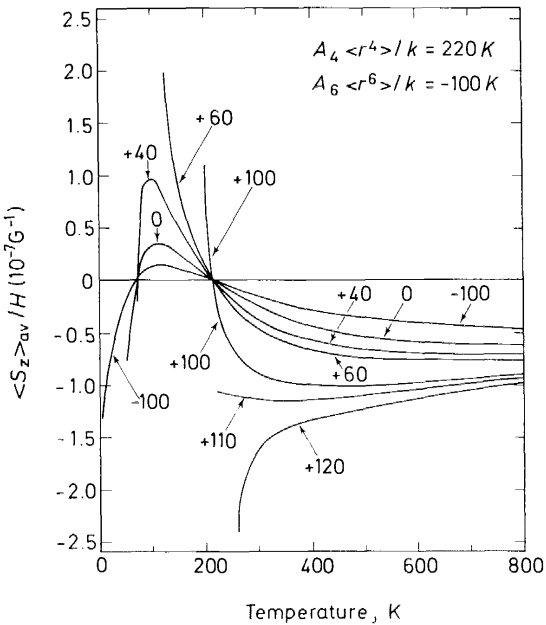


Figure 10. Effect of exchange interaction on $\langle S_z \rangle_{av}/H$ of Sm^{3+} ion in a cubic crystal field with $A_4 \langle r^4 \rangle / k = 220 K$ and $A_6 \langle r^6 \rangle / k = -100 K$. The curves are labelled with the values of J_{ff}/k in Kelvin.

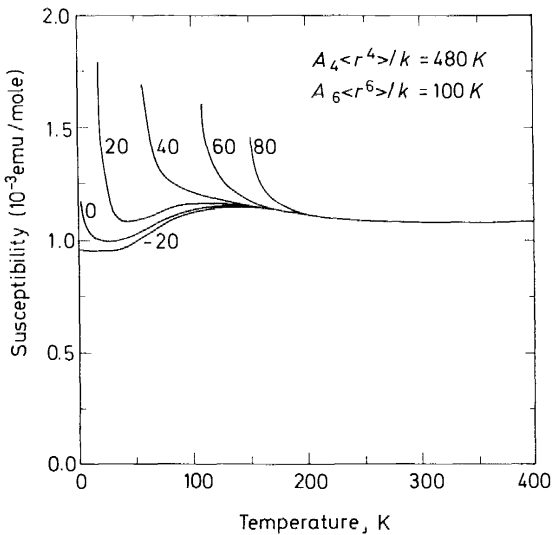


Figure 11. Effect of exchange interaction on the susceptibility of the Sm^{3+} ion in a cubic crystal field with $A_4 \langle r^4 \rangle / k = 480 K$ and $A_6 \langle r^6 \rangle / k = 100 K$. The curves are labelled with the values of J_{ff}/k in Kelvin.

antiferromagnetic exchange interaction (negative \mathcal{J}_{ff}) decreases the magnitudes of χ_f and $\langle S_z \rangle_{av}/H$.

Experimental results and discussion

Though nuclear magnetic resonance of the non-magnetic constituent has been studied in several samarium compounds such as SmX ($X = \text{P, As, Sb, Bi}$)^{38,39}, SmAl_3 ⁴⁰, SmAl_2 ⁴², SmF_3 ⁴⁴, SmSn_3 ^{20,21,41,43}, SmPt_2 ⁴¹, etc., we shall confine our discussions here to SmSn_3 and SmPt_2 . The compound SmSn_3 (isostructural to CeSn_3) has the cubic Cu_3Au type of crystal structure. The susceptibility of SmSn_3 was originally measured by Tsuchida and Wallace¹³ in the temperature range of 4.2–300 K. They observed that SmSn_3 orders antiferromagnetically with $T_N = 12$ K. Recently de Wijn *et al.*⁵⁵ have also measured its susceptibility from 4.2 to 850 K ($T_N = 11$ K) and their results are shown in Figure 12. The ^{119}Sn Knight shift in SmSn_3 has been

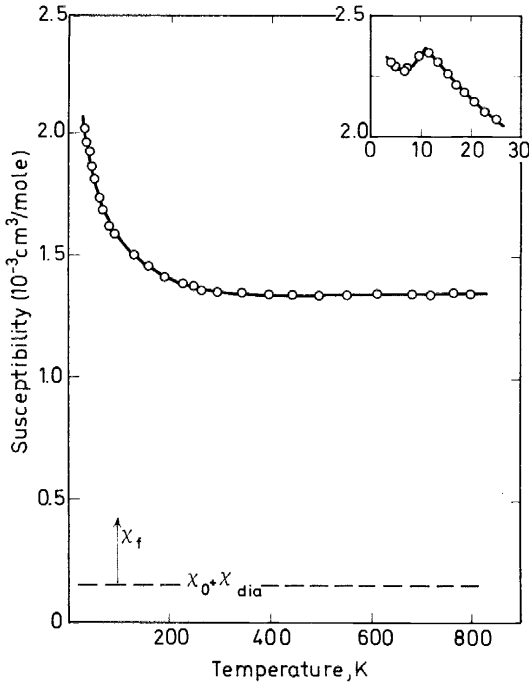


Figure 12. Magnetic susceptibility of SmSn_3 versus the temperature from ref. 55.

measured by Rao and Vijayaraghavan^{20,43}, by Borsa *et al.*²¹, and by Malik⁴¹ in the temperature region 77–300 K from which it has been found that the crossover in K_f , the 4f contribution to the ^{119}Sn Knight shift, is completely absent. These measurements have now been extended down to the magnetic ordering temperature by the present authors. The procedure used for observing the n.m.r. has been described earlier in connection with the Sn n.m.r. measurements in CeSn_3 . The results of the present measurements of the Sn

Knight shift in SmSn_3 are shown in *Figure 13* and it is found that no crossover in K_f occurs between 15–300 K.

The compound SmPt_2 (isostructural to CePt_2) has the cubic Laves phase structure. The ^{195}Pt Knight shift in SmPt_2 has been reported by Malik⁴¹ (*Figure 14*) in the temperature region 100–350 K and the crossover tempera-

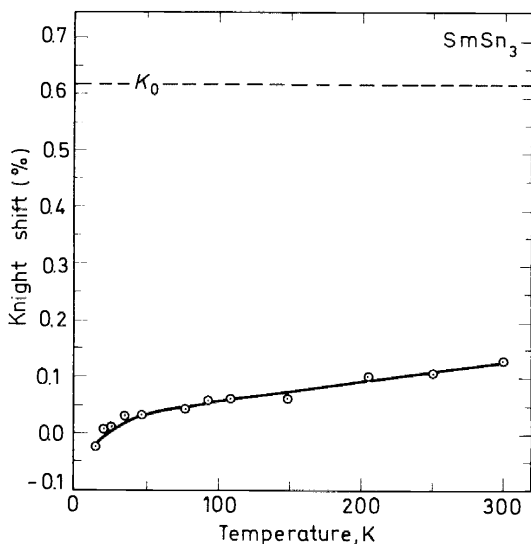


Figure 13. The ^{119}Sn Knight shift in SmSn_3 versus the temperature (present work).

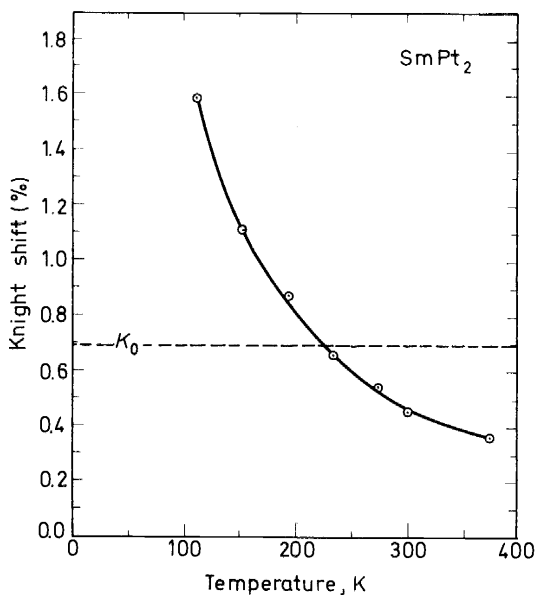


Figure 14. The ^{195}Pt Knight shift in SmPt_2 versus the temperature.

ture has been found to be 230 ± 20 K. This is the only system so far where a reduced T_{co} (compared to the value of 300 K in the free Sm^{3+} ion) has been observed. The compound SmPt_2 has been found to order ferromagnetically with $T_c = 16$ K and its susceptibility has been measured from 300 K up to the magnetic ordering temperature⁵⁶. The results of the magnetic susceptibility of SmPt_2 are shown in *Figure 15*. The magnetic moment per samarium ion at 1.2 K has been found to be $0.19 \mu_B$, which is considerably smaller than the free ion value ($0.71 \mu_B$).

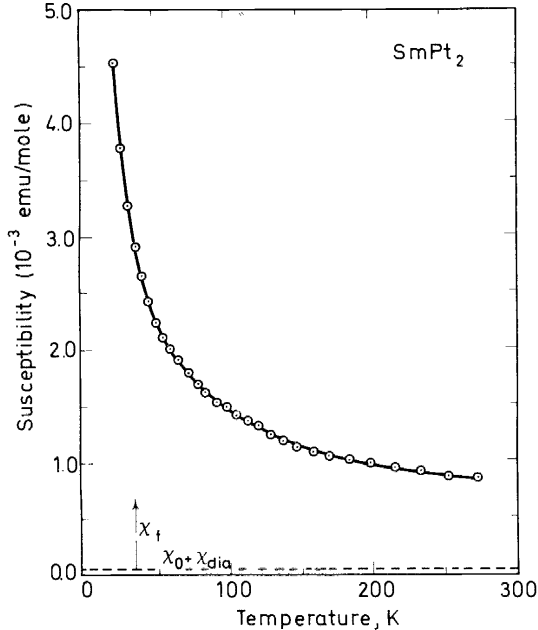


Figure 15. The magnetic susceptibility of SmPt_2 versus the temperature (unpublished results of S. K. Malik, R. Vijayaraghavan, S. G. Sankar and V. U. S. Rao).

The magnetic susceptibility and the Knight shift results in SmSn_3 (the latter in the temperature region 77–300 K) have been analysed by Malik⁷ and by de Wijn *et al.*⁵⁵ in terms of the crystal field effects. The latter authors have obtained a range of values of the crystal field parameters $A_4\langle r^4 \rangle$ and $A_6\langle r^6 \rangle$ which simultaneously fit the susceptibility and the Knight shift results. With the present extension of the Sn Knight shift measurements down to the magnetic ordering temperature it is possible to narrow down the range of crystal field parameters. We have calculated $\langle S_z \rangle_{av}/H$ for the range of values of $A_4\langle r^4 \rangle/k$ and $A_6\langle r^6 \rangle/k$ reported in ref. 55 and using a value of -25 K for the exchange interaction constant \mathcal{J}_{ff}/k . In order to calculate K_f , we used the K_0J_{sf} values obtained by fitting the experimental K_f values in SmSn_3 in the temperature region 77–300 K as was done in ref. 55. Some of the calculated K_f values for ^{119}Sn in SmSn_3 are plotted in *Figure 16* as a function of temperature along with the experimentally observed values. It is found that the range of values reported earlier⁵⁵ where $A_4\langle r^4 \rangle$ is negative

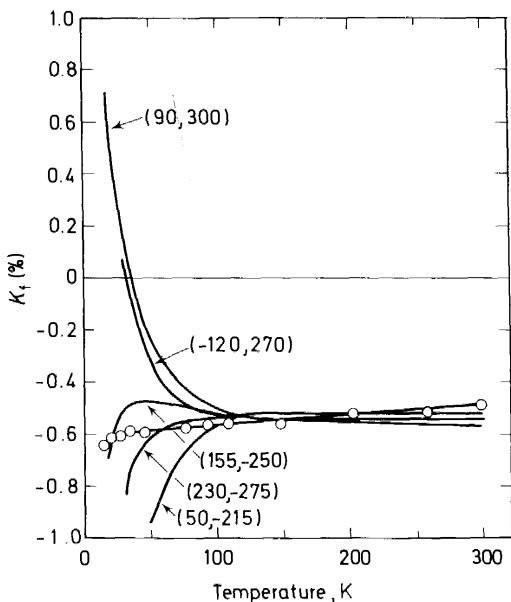


Figure 16. The 4f contribution K_f to the ^{119}Sn Knight shift in SmSn_3 versus the temperature. The other curves are the calculated K_f values using \mathcal{J}_{ff}/k and the crystal field parameters suggested⁵⁵ for SmSn_3 . The numbers in parentheses are the values of $A_4\langle r^4 \rangle/k$ and $A_6\langle r^6 \rangle/k$ in Kelvin.

and $A_6\langle r^6 \rangle$ positive (upper left quadrant of Figure 5 in ref. 55) all yield a crossover close to 40 K and can be ruled out as inappropriate to SmSn_3 in view of the present extended Knight shift results. Similarly not all the values of $A_4\langle r^4 \rangle$ and $A_6\langle r^6 \rangle$ in the second range of ref. 55 are applicable to SmSn_3 . The calculations are under way to determine the range of crystal field parameters which fit the present experimental results. The Knight shift and susceptibility results on SmPt_2 are also being analysed.

Electron paramagnetic resonance g shift of Gd^{3+} in the presence of Sm^{3+}

Several years ago Shaltiel *et al.*⁵⁷ investigated the paramagnetic resonance g shift to be expected of a system A of paramagnetic ions dissolved in a metallic host matrix in which a small concentration of a second species of paramagnetic ions, system B is also dissolved. The spins S_a and S_b of the systems A and B, respectively, interact with the conduction electron spins through an exchange interaction of the type $-\bar{J}_n S_n \cdot s$ ($n = a$ or b and $\bar{J}_n = J_{sf}$). The polarization induced in the conduction band of the host by the spins of the system A is sensed by the spins of the system B and vice-versa. In particular, Shaltiel *et al.*⁵⁷ discuss the case where the system A consists of Gd^{3+} ions whose paramagnetic resonance can be observed and system B consists of other rare earth ions. The additional g shift of Gd due to the presence of system B of rare earth ions is given by⁵⁷

$$\Delta g_B = \Delta g_0 \bar{J}_b (g_{Jb} - 1) \chi_b c_B / g_e g_{Jb} \mu_B^2 \quad (33)$$

where χ_b and c_B are respectively the susceptibility per rare earth ion and the atomic concentration of the B system. The shift Δg_0 given by

$$\Delta g_0 = \bar{J}_a \chi_0 V / g_e n_0 \mu_B^2 \quad (34)$$

is the g shift of Gd alone in the host metal and is proportional to χ_0 , the susceptibility of the host metal. Equation 33 for the additional g shift is analogous to the expression for the additional Knight shift, e.g. equation 8, due to the presence of rare earth ions, and Δg_0 plays the role of K_0 .

In the palladium metal host, Shaltiel *et al.* found Δg_0 to be negative implying negative exchange interaction \bar{J}_a . Further, they observed that the additional g shift Δg_B was negative for rare earths to the left of Gd, and positive for the rare earths to the right of Gd in the Periodic Table. The change in the sign of Δg_B is due to the fact that the factor $(g_{J_b} - 1)$ occurring in equation 33 changes sign from negative to positive as one goes from rare earths to the left of Gd to rare earths to the right of Gd. The measurements yield a negative value for \bar{J}_b too. The Gd/ g values in the presence of various RE are plotted as a function of temperature in Figure 17. Samarium was found to behave anomalously. The shift Δg_B in $\text{Pd}_{0.96}\text{Gd}_{0.02}\text{Sm}_{0.02}$ is positive which is opposite to what is expected on the basis of the above model and, moreover, its temperature dependence does not conform to

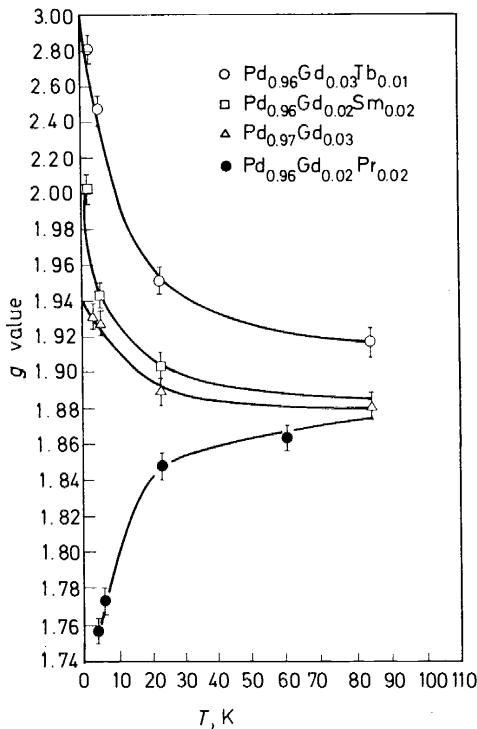


Figure 17. Paramagnetic resonance g value of Gd in the alloys $\text{Pd}_{0.96}\text{Tb}_{0.01}\text{Gd}_{0.03}$, $\text{Pd}_{0.96}\text{Sm}_{0.02}\text{Gd}_{0.02}$; $\text{Pd}_{0.97}\text{Gd}_{0.03}$; $\text{Pd}_{0.96}\text{Gd}_{0.02}\text{Pr}_{0.02}$; versus the temperature.

what would be expected from the temperature-dependent part of the susceptibility of samarium. It is now possible to understand this anomalous behaviour of the additional g shift due to samarium in terms of the crystal field effects.

First of all it may be pointed out that equation 33 has been obtained after replacing $\langle S_{bz} \rangle_{av}/H$ by $-(g_{Jb} - 1)\chi_v/g_{Jb}\mu_B$. However, as pointed out at the beginning, the linear relation between $\langle S_z \rangle_{av}$ and χ is not valid in the case of Sm^{3+} ions. Therefore, it is more appropriate to write Δg_B due to Sm^{3+} ions as

$$\Delta g_B = -\Delta g_0 \bar{J}_b \langle S_{bz} \rangle_{av} / g_c \mu_B H \quad (35)$$

Once it is recognized that Δg_B is proportional to the spin average of the rare earth ion it is easy to understand the behaviour of Δg_B in $\text{Pd}_{0.96}\text{Gd}_{0.02}\text{Sm}_{0.02}$. The palladium metal has a cubic crystal structure and if Sm^{3+} ions go substitutionally in Pd, they would be subjected to crystal fields of cubic symmetry. The effect of cubic crystal fields on $\langle S_z \rangle_{av}$ of Sm^{3+} ion has been discussed earlier where it has been shown that the White-Van Vleck type of crossover in $\langle S_z \rangle_{av}/H$ may be suppressed because of crystal fields so that $\langle S_z \rangle_{av}/H$ is negative throughout. We suggest that the crystal fields in $\text{Pd}_{0.96}\text{Gd}_{0.02}\text{Sm}_{0.02}$ are strong enough to suppress the crossover in $\langle S_z \rangle_{av}/H$ of Sm^{3+} and make it negative at all temperatures. Since Δg_0 is negative, a negative \bar{J}_b would make Δg_B positive throughout as has been observed. Thus it is possible to get at least the right sign of \bar{J}_b consistent with that obtained for other rare earth ions. A detailed analysis of Δg_B in terms of the crystal field interactions is underway⁵⁸.

The 4f-induced hyperfine field at a samarium nuclear site in paramagnetic state

So far we have discussed the contribution of the 4f electrons to the Knight shift of a non-magnetic site and to the paramagnetic resonance g shift of Gd^{3+} . Both the Knight shift and the g shift were found to be proportional to $\langle S_z \rangle_{av}$ of the Sm^{3+} ion. Let us now examine the hyperfine field produced by the 4f electrons at the samarium nuclear site itself in the presence of an externally applied field. The orbital and the spin-dipolar contribution to the hyperfine field due to 4f electrons may be written in the operator form as⁵⁹

$$H_{op}^{4f} = -2\mu_B \sum_i \{r_i^{-3} [L_i - s_i + 3r_i(r_i \cdot s_i)/r_i^2]\} \quad (36)$$

where the summation is over all the 4f electrons. The matrix elements of H_{op}^{4f} between various states of the Hund's rule ground multiplet arising from a given $4f^N$ configuration have been discussed in the literature^{37, 60, 61}. Since H_{op}^{4f} is a vector, it follows from the Wigner-Eckart theorem that its matrix elements in the (SLJM) representation are related to the matrix elements of the magnetic moment operator ($\mathbf{L} + 2\mathbf{S}$). Therefore, for the z component of the hyperfine field operator, we can write

$$\langle \text{SLJM} | H_{op,z}^{4f} | \text{SLJM} \rangle = -2\mu_B \langle r^{-3} \rangle M \langle J || N || J \rangle \quad (37)$$

and

$$\langle \text{SLJM} | H_{op,z}^{4f} | \text{SLJ} - 1 M \rangle = -2\mu_B \langle r^{-3} \rangle [J^2 - M^2]^{\frac{1}{2}} \langle J || N || J - 1 \rangle \quad (38)$$

where the radial integration over the 4f wave function is supposed to have

been carried out, and $\langle r^{-3} \rangle$ is the expectation value of the inverse cube radius of the 4f electron orbital. The multiplicative factors $\langle J \| N \| J \rangle$ and $\langle J \| N \| J - 1 \rangle$ for the Hund's rule ground multiplet are given by

$$\begin{aligned} \langle J \| N \| J \rangle &= \frac{J(J+1) + L(L+1) - S(S+1)}{2J(J+1)} \\ &+ v \frac{g_s}{2} \left\{ 3J(J+1) - 2L(L+1) - 3S(S+1) \right. \\ &\left. - \frac{[3J(J+1) - L(L+1) + S(S+1)][3J(J+1) - L(L+1) - 3S(S+1)]}{4J(J+1)} \right\} \end{aligned} \quad (39)$$

$$\begin{aligned} \langle J \| N \| J - 1 \rangle &= - \left\{ 1 + \frac{v g_s}{2} [3J^2 - L(L+1) - 3S(S+1)] \right\} \\ &\times \left[\frac{[(S+L+1)^2 - J^2][J^2 - (S-L)^2]}{4J^2(2J+1)(2J-1)} \right]^{\frac{1}{2}} \end{aligned} \quad (40)$$

with

$$v = \frac{4S - (2l + 1)}{(2l - 1)(2l + 3)S(2L - 1)} \quad (41)$$

and $l = 3$ for f electrons. An expression for $\langle H_z^{4f} \rangle_{av}/H$ for the free Sm^{3+} ion in the presence of an external field is given in ref. 37, and the one in the presence of an external and exchange fields has been obtained by Malik⁶². It is found that in the case of the free Sm^{3+} ion $\langle H_z^{4f} \rangle_{av}/H$ is not proportional to χ_f , and, moreover, it remains positive throughout, unlike $\langle S_z \rangle_{av}/H$, i.e. $\langle H_z^{4f} \rangle/H$ does not pass through zero at any temperature⁶³.

The effects of crystal fields of cubic symmetry, and the exchange fields, on the 4f-induced hyperfine field on samarium nucleus have been investigated by Malik and Vijayaraghavan⁶⁴. Treating the exchange interaction as a perturbation over the eigenfunctions $|m\rangle$ and the energy eigenvalues $E_m^{(0)}$ obtained after diagonalizing the Hamiltonian of equations 22, we obtain the following expression

$$\langle H_z^{4f} \rangle_{av} = \langle H_z^{4f} \rangle_{av}^0 + 2\mu_B H_{ex} \sigma_{S, H^{4f}} \quad (42)$$

For the case where the exchange interaction is given by the molecular field approximation (equation 30) we have

$$\frac{\langle H_z^{4f} \rangle_{av}}{H} = \frac{\langle H_z^{4f} \rangle_{av}^0}{H} - \left[\frac{\mathcal{J}_{ff} \sigma_{S, H^{4f}}}{1 + \mathcal{J}_{ff} \sigma_{S, S}} \right] \frac{\langle S_z \rangle_{av}^0}{H} \quad (43)$$

where $\sigma_{A, B}$ is given by equation 29 and superscript 0 denotes the corresponding value in the absence of exchange. For the sake of brevity we shall denote $\langle H_z^{4f} \rangle_{av}$ by H_{4f} . The quantity H_{4f}/H , which may also be termed the 4f contribution to the Knight shift of the samarium nucleus, has been calculated

as a function of temperature for a wide range of crystal field parameters $A_4\langle r^4 \rangle$ and $A_6\langle r^6 \rangle$, and the exchange constant \mathcal{J}_{ff} . The experimentally estimated value by Bleaney⁶⁵ has been used for $\langle r^3 \rangle$. In Figure 18, the temperature dependence of H_{4f}/H is shown for a few typical values of $A_4\langle r^4 \rangle$ and $A_6\langle r^6 \rangle$ in the absence of exchange. The curves are labelled with the values of $A_4\langle r^4 \rangle/k$ and $A_6\langle r^6 \rangle/k$ in Kelvin. In the case of the free Sm^{3+} ion, H_{4f}/H is positive throughout (curve marked free ion in Figure 18). However, as the crystal field strength is changed, either by changing $A_6\langle r^6 \rangle$ with $A_4\langle r^4 \rangle$ constant (solid curves in Figure 18) or by changing $A_4\langle r^4 \rangle$ with $A_6\langle r^6 \rangle$ constant (dotted curves in Figure 18), H_{4f}/H shows a sign reversal and becomes negative at low temperatures. For some combinations of crystal field parameters more than one sign reversal may occur.

The effect of exchange interaction between samarium ions on H_{4f}/H in the presence of crystal fields is shown in Figures 19 and 20. In Figure 19 we have plotted H_{4f}/H for $A_4\langle r^4 \rangle/k = -320$ K and $A_6\langle r^6 \rangle/k = -200$ K and \mathcal{J}_{ff} is varied. In the absence of the exchange interaction ($\mathcal{J}_{ff} = 0$) there is one crossover in H_{4f}/H . However, positive values of \mathcal{J}_{ff} (ferromagnetic exchange interaction) raise the crossover temperature while negative values of \mathcal{J}_{ff} lower the crossover temperature and eventually suppress the crossover. In Figure 20 the effect of exchange interaction on H_{4f}/H is shown for another set of crystal field parameters, namely, $A_4\langle r^4 \rangle/k = A_6\langle r^6 \rangle/k = 200$ K. For $\mathcal{J}_{ff} = 0$ there is no crossover in H_{4f}/H . However, it is to be noted from the figure that depending upon its strength a ferromagnetic exchange interaction may induce one or more crossovers in H_{4f}/H . Thus we see that both the

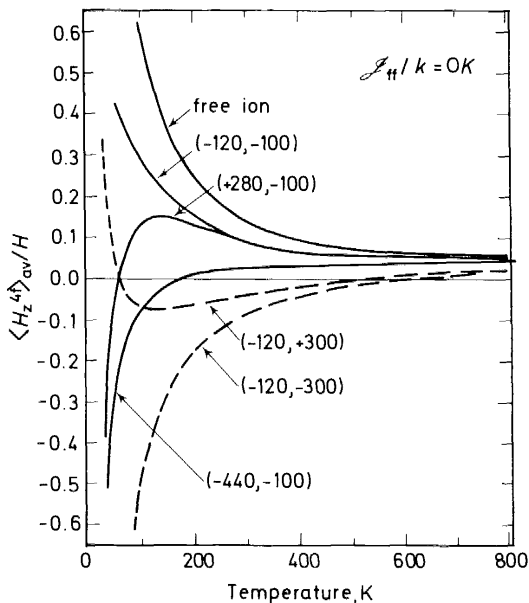


Figure 18. Effect of variation of $A_6\langle r^6 \rangle$ (solid curves) and $A_4\langle r^4 \rangle$ (dotted curves) on the 4f-induced hyperfine field $\langle H_z^{4f} \rangle_{av}/H$ at samarium nuclear site in a cubic crystal field. The numbers in parentheses are respectively the values of $A_4\langle r^4 \rangle/k$ and $A_6\langle r^6 \rangle/k$ in Kelvin.

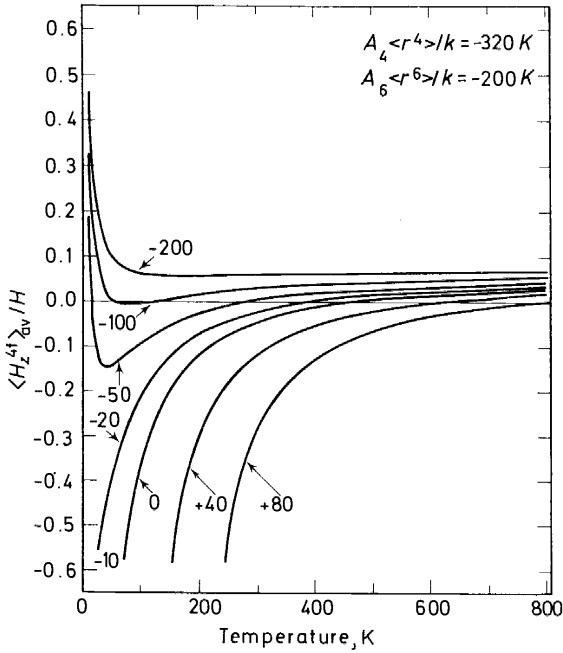


Figure 19. Effect of exchange interaction on the 4f-induced hyperfine field $\langle H_z^{4f} \rangle_{av}/H$ at samarium nuclear site in a cubic crystal field with $A_4 \langle r^4 \rangle / k = -320 \text{ K}$ and $A_6 \langle r^6 \rangle / k = -200 \text{ K}$. The curves are labelled with the values of \mathcal{J}_{ff}/k in Kelvin.

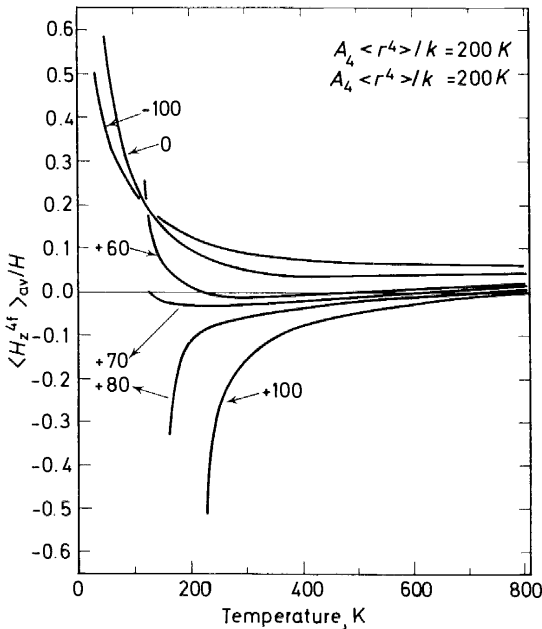


Figure 20. Effect of exchange interaction on the 4f-induced hyperfine field $\langle H_z^{4f} \rangle_{av}/H$ at samarium nuclear site in a cubic crystal field with $A_4 \langle r^4 \rangle / k = A_6 \langle r^6 \rangle / k = 200 \text{ K}$. The curves are labelled with the values of \mathcal{J}_{ff}/k in Kelvin.

crystal fields and the exchange interaction considerably influence the temperature dependence of H_{4f}/H .

Though the n.m.r. of samarium in paramagnetic compounds has not been observed so far, the kind of effects mentioned above can be easily studied by measuring, using perturbed angular correlation (PAC), the paramagnetic correction factor³⁷ β , which is the ratio of the effective field H_{eff} seen by the nucleus to the applied field H . In the case of rare earth ions, neglecting small contributions to H_{eff} such as those arising from the core polarization and the conduction electron polarization, we can write $\beta = 1 + H_{4f}/H$. Recently Tandon *et al.*⁶⁶ have reported, using the PAC technique, what appears to be the first observation of negative H_{4f}/H on a samarium nucleus. The measurements were carried out on paramagnetic EuAl_2 in which ^{152}Eu activity was produced by neutron irradiation. The ^{152}Eu decays to levels in ^{152}Sm , and 1408–122 keV gamma cascade ($2^- \rightarrow 2^+ \rightarrow 0^+$) was used. The directional correlation and the mean precession angle $\omega\tau$ (in the presence of an external field) were measured at various temperatures. The observed β values are 0.89 ± 0.11 , 0.08 ± 0.10 , -1.45 ± 0.25 at temperatures of 300 K, 200 K and 85 K respectively, from which it is to be noted that H_{4f}/H is negative at all temperatures of measurements.

Hyperfine field on samarium nucleus and the saturation magnetic moment on samarium ion in ferromagnetic compounds

In the previous section it was shown that in paramagnetic samarium compounds the hyperfine field H_{4f}/H at the samarium nuclear site induced by the paramagnetism of 4f electrons may change its sign at one or more temperatures because of the mixing of ionic J levels of Sm^{3+} ion by crystal fields and exchange fields, while in the case of the free Sm^{3+} ion H_{4f}/H is positive at all temperatures. In this section we extend the calculations to the ferromagnetic region and calculate the hyperfine field⁶⁷ on samarium nucleus and the saturation magnetic moment^{68–71} (electronic) on the samarium ion.

In general, the hyperfine field on the samarium nucleus in any ferromagnetic compound and also the electronic magnetic moment is a function of several parameters, such as the crystalline electric field, the exchange field, the angle which the exchange field or the easy direction of magnetization makes relative to the local crystal field axis, etc. Since these parameters vary from one compound to another, each system has to be discussed individually. However, in order to demonstrate the effects of crystal fields on H_{4f} , we consider the case of a cubic ferromagnetic samarium compound in which Sm^{3+} ions occupy a site of local cubic symmetry. Further, we assume [001] to be the easy direction of magnetization. Therefore, the exchange field points along [001] which we take as the quantization or the z axis. The cubic crystal field Hamiltonian for $z \parallel [001]$ is given by equation 18. In the ferromagnetic state the exchange field is very large and cannot be treated as a perturbation over the crystal field Hamiltonian. Therefore, we now diagonalize the Hamiltonian

$$\mathcal{H} = \lambda \mathbf{L} \cdot \mathbf{S} + \mathcal{H}_C + 2\mu_B H_{\text{ex}} S_z + \mu_B H (L_z + 2S_z) \quad (44)$$

to obtain the energy eigenvalues E_m and the eigenfunctions $|m\rangle$ and calculate the Boltzmann average of the expectation value of the z component of the hyperfine field operator given by equation 36.

We confine our calculations to ferromagnetic samarium compounds with non-magnetic elements, so that the exchange interaction responsible for magnetic ordering is between Sm^{3+} spins. In the molecular field approximation, the exchange field which the Sm^{3+} ions exert on each other is given by $2\mu_B H_{\text{ex}} = -\mathcal{J}_{\text{ff}} \langle S_z \rangle_{\text{av}}$, where \mathcal{J}_{ff} is the exchange interaction constant, and $\langle S_z \rangle_{\text{av}}$ is the thermal average of the Sm^{3+} spin. Typically we take $\mathcal{J}_{\text{ff}}/k = 70$ K which yields a Curie temperature of about 120 K, though dependent slightly on the crystal field parameters. Although H_{ex} is proportional to $\langle S_z \rangle_{\text{av}}$, the latter itself depends implicitly on H_{ex} through the eigenfunctions and the energy eigenvalues (used in the calculation of expectation values and Boltzmann averaging) obtained after diagonalizing the Hamiltonian of equation 44 containing H_{ex} . Thus the exchange field is to be determined self-consistently for a given value of \mathcal{J}_{ff} , for each set of crystal field parameters $A_4 \langle r^4 \rangle$ and $A_6 \langle r^6 \rangle$ and for each temperature. To accomplish this we start with $H_{\text{ex}} = 0$, $H = 10$ kOe, diagonalize the Hamiltonian of equation 44 for some combination of $A_4 \langle r^4 \rangle$ and $A_6 \langle r^6 \rangle$, calculate $\langle S_z \rangle_{\text{av}}$ and thus H_{ex} . This value of H_{ex} is used in the next iteration and the process repeated till self-consistent values of $\langle S_z \rangle_{\text{av}}$ or H_{ex} are obtained. This completely determines the Hamiltonian and various quantities of interest can be calculated. The external field H is used to determine the sign of H_{4f} , i.e. if H_{4f} is parallel to H it is taken to be positive and if H_{4f} is antiparallel to H it is taken to be negative.

The hyperfine field on samarium has been calculated at 0 K for a range of crystal field parameters $A_4 \langle r^4 \rangle$ and $A_6 \langle r^6 \rangle$. Figure 21 shows the plot of H_{4f} versus $A_4 \langle r^4 \rangle$ and the curves are labelled with the values of $A_6 \langle r^6 \rangle/k$ in

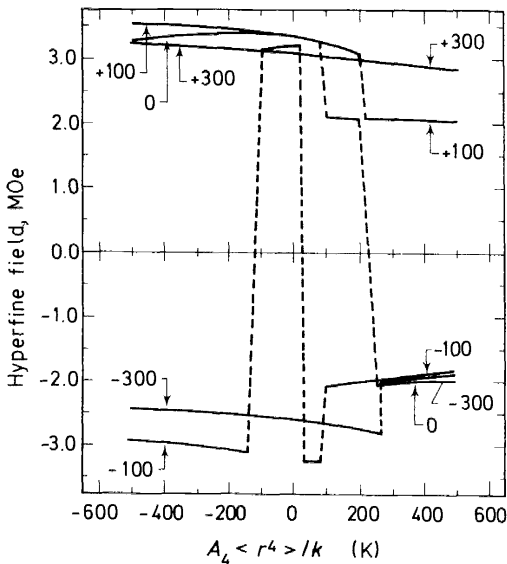


Figure 21. The variation of the 4f-induced hyperfine field at samarium nuclear site in the ferromagnetic state as a function of $A_4 \langle r^4 \rangle/k$ and $A_6 \langle r^6 \rangle/k$, the parameters of the cubic crystal field. The curves are labelled with the values of $A_6 \langle r^6 \rangle/k$ in Kelvin. Throughout $H_{\text{ex}} \parallel [001]$ and $\mathcal{J}_{\text{ff}}/k = +70$ K.

Kelvin. In the case of the free Sm^{3+} ion we have $H_{4f} \approx 3.37$ MOe (throughout we refer to H_{4f} values at 0 K). It is to be noted from *Figure 21* that depending upon the parameters $A_4\langle r^4 \rangle$ and $A_6\langle r^6 \rangle$ the crystal fields bring about (i) a reduction in H_{4f} , (ii) an enhancement in H_{4f} to the extent of ten per cent over the free ion value, and (iii) a change in the sign of H_{4f} . (The dotted lines correspond to sudden changes in H_{4f} as a function of $A_4\langle r^4 \rangle$.) However, unlike in the paramagnetic state, H_{4f} does not show any crossover as a function of temperature in the ferromagnetic state. In most other rare earth ions, the crystal fields cause only a reduction in H_{4f} from the free ion value. The other two effects, namely, the enhancement and the sign change in H_{4f} are peculiar to the Sm^{3+} ion and arise because of the admixture of excited ionic J levels into its ground level by crystal fields. Though we have considered a particular case of a cubic samarium compound with $H_{\text{ex}} \parallel [001]$, similar behaviour is expected when H_{ex} is along some other direction or even when Sm^{3+} ions occupy sites of other than cubic symmetry. However, the regions where H_{4f} is negative would depend on these details. Thus one cannot assume H_{4f} on samarium to be positive unless an explicit determination of its sign is carried out. It may be remarked that the hyperfine field on the non-magnetic site in samarium compounds, which is proportional to $\langle S_z \rangle_{\text{av}}$, is also strongly influenced by crystal fields, both in magnitude and sign. Experimental determination of the sign and magnitude of H_{4f} on samarium in a few compounds is in progress.

The effects of cubic crystal fields on the saturation magnetic moment on samarium in ferromagnetic compounds have also been investigated⁶⁸⁻⁷⁰. As discussed earlier, in ferromagnetic samarium compounds with non-magnetic elements the exchange field H_{ex} acting on Sm^{3+} ions is to be determined self-consistently. However, in ferromagnetic samarium compounds with magnetic elements the dominant exchange interaction experienced by samarium ions is with other magnetic ions and not with other samarium ions. Therefore, the exchange field acting on Sm^{3+} ions in this case is an impressed one⁷² and does not have to be determined self-consistently. The magnetic moment is defined as

$$\mu = -\mu_B \sum_m \langle m | L_z + 2S_z | m \rangle \exp(-E_m/kT) / \sum_m \exp(-E_m/kT) \quad (45)$$

where E_m and $|m\rangle$ are, respectively, the energy eigenvalues and eigenfunctions of the Hamiltonian given by equation 44. In order to demonstrate the effects of cubic crystal fields on the saturation magnetic moment on samarium in compounds with non-magnetic elements we again take $\mathcal{J}_{\text{ff}}/k = 70$ K and assume $[001]$ as the easy direction of magnetization. The calculated values of the saturation magnetic moment as a function of $A_4\langle r^4 \rangle$ and $A_6\langle r^6 \rangle$ are shown in *Figure 22* in which the curves are labelled with the values of $A_6\langle r^6 \rangle/k$ in Kelvin. It is to be noted that even in free Sm^{3+} ion ($A_4\langle r^4 \rangle/k = A_6\langle r^6 \rangle/k = 0$), the saturation magnetic moment is less than $g_J J = 0.71$ because of the mixing of the higher J levels into the ground level of Sm^{3+} by exchange fields. An expression for the saturation moment on the free Sm^{3+} ion taking into account the admixture of $J = \frac{7}{2}$ level into $J = \frac{5}{2}$ level by exchange fields has been obtained by Stewart⁷¹, who has also shown the importance of the conduction electron polarization contribution to the total magnetic moment

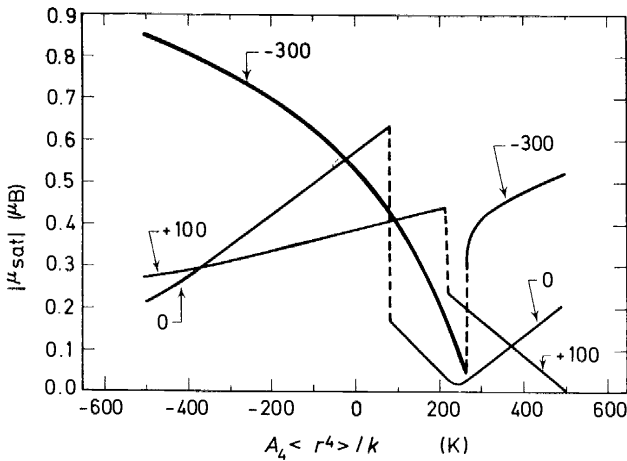


Figure 22. The variation of the saturation magnetic moment of Sm^{3+} ion in the ferromagnetic state as a function of $A_4 \langle r^4 \rangle / k$ and $A_6 \langle r^6 \rangle / k$, the parameters of the cubic crystal field. The curves are labelled with the values of $A_6 \langle r^6 \rangle / k$ in Kelvin. Throughout $H_{\text{ex}} \parallel [001]$ and $\mathcal{J}_{\text{ff}} / k = +70$ K.

in ferromagnetic samarium compounds as well as to the susceptibility and the spin average of the Sm^{3+} ion⁷³. It is to be noted from Figure 22 that the crystal fields, in general, tend to quench the magnetic moment from the free ion value^{74, 75}. (This reduction is over and above that caused by the exchange field alone.) However, it is interesting to note that in some cases the crystal fields cause an enhancement over the free ion value^{74, 75}. Similar results are obtained⁶⁸⁻⁷⁰ for the magnetic moment in ferromagnetic compounds with magnetic elements. The results for the particular case where $|\mu_B H_{\text{ex}} / k| = 25$ K and $[001]$ is the easy direction of magnetization are shown in Figure 23.

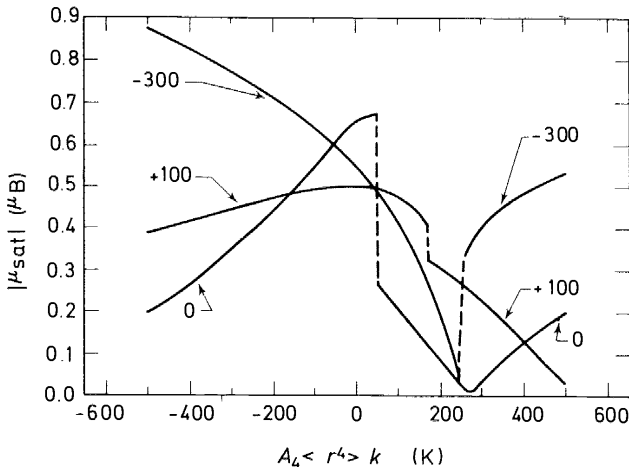


Figure 23. The variation of the saturation magnetic moment of Sm^{3+} ion in the ferromagnetic state as a function of $A_4 \langle r^4 \rangle / k$ and $A_6 \langle r^6 \rangle / k$, the parameters of the cubic crystal field. The curves are labelled with the values of $A_6 \langle r^6 \rangle / k$ in Kelvin. Throughout $H_{\text{ex}} \parallel [001]$ and $|\mu_B H_{\text{ex}} / k| = 25$ K.

Another interesting feature which emerges from these calculations for ferromagnetic samarium compounds either with magnetic or with non-magnetic elements is that for some values of crystal field parameters the calculated magnetic moment $\vec{\mu}_{\text{Sm}}$ is parallel to $\langle S_z \rangle_{\text{av}}$ (thin curves in *Figures 22* and *23*) while for some other crystal field parameters $\vec{\mu}_{\text{Sm}}$ is antiparallel to $\langle S_z \rangle_{\text{av}}$ (thick curves in *Figures 22* and *23*, and dotted lines in both the figures correspond to sudden changes in μ_{Sm} as a function of $A_4 \langle r^4 \rangle / k$). For the rare earth (RE) ions $\mu_{\text{RE}} = -\mu_{\text{B}}(L_z + 2S_z)$ is parallel (antiparallel) to S for ions having $J = L - S$ ($J = L + S$). Thus it appears that for some strength of crystal fields the Sm^{3+} ion may behave effectively like an $(L + S)$ ion rather than an $(L - S)$ ion. This indeed seems to be so in ferromagnetic samarium compounds with some transition elements (TE). The sublattice coupling between μ_{RE} and μ_{TE} is ferromagnetic (antiferromagnetic) for RE belonging to the first half (second half)^{74, 75}. However, μ_{Sm} seems to couple antiferromagnetically with μ_{TE} in SmFe_2 , $\text{Sm}_2\text{Co}_{17}$ and SmCo_5 . Thus crystal fields might be responsible for the anomalous behaviour of samarium in the above mentioned compounds and also possibly in $\text{Sm}_6\text{Mn}_{23}$ ^{74, 75}.

The crystal field effects on the temperature dependence of the sublattice magnetization of samarium (particularly in samarium compounds with magnetic elements) have also been investigated. It was pointed out by White and Van Vleck³⁶ that in ferromagnetic samarium compounds in which the Sm^{3+} ion could be considered as a 'free' ion, the exchange field acting alone produces a sign reversal, or a crossover, in the magnetization M_{Sm} of Sm^{3+} ion at a temperature of about 300 K. The crossover in the magnetization arises because of the admixture of higher J levels of Sm^{3+} into its ground level by exchange fields. The crossover temperature T_{co} where M_{Sm} of the free ion changes sign is independent of the magnitude of H_{ex} as well as independent of the Curie temperature of the system. (Of course, it is assumed throughout that $T_{\text{C}} > T_{\text{co}}$.) Recent calculations by Malik and Vijayaraghavan⁷⁶ show that the crystal fields may considerably reduce the crossover temperature in M_{Sm} ($M_{\text{Sm}} = -N\mu_{\text{B}}\langle L_z + 2S_z \rangle_{\text{av}}$) from the value of 300 K in the free ion. In some cases crystal fields may bring about more than one crossover or completely suppress the crossover in M_{Sm} . In ferromagnetic samarium compounds with non-magnetic elements the crystal fields cause additional anomalies in M_{Sm} , such as a broad maximum in the M_{Sm} versus T curve.

The only system so far in which a crossover in M_{Sm} has been observed is samarium iron garnet ($\text{Sm}_3\text{Fe}_5\text{O}_{12}$, $T_{\text{C}} = 560$ K). The crossover temperature has been obtained by comparing the magnetization of $\text{Sm}_3\text{Fe}_5\text{O}_{12}$ (SmIG) and $\text{Y}_3\text{Fe}_5\text{O}_{12}$ (YIG) in the latter of which yttrium is non-magnetic and the total magnetization comes from Fe ions. Therefore, $M_{\text{SmIG}} - M_{\text{YIG}}$ gives the contribution of M_{Sm} to the total magnetization. However, M_{Sm} even in the free ion is so small that early measurements failed to detect it at all⁷⁷⁻⁷⁹. Consequently very careful measurements by Perel and Schieber⁸⁰ on polycrystalline materials and by Nowlin⁸¹, Geller *et al.*⁸² and Harrison *et al.*⁸³ on single crystal materials showed the existence of a crossover in M_{Sm} and Geller *et al.*⁸² gave a value of 300 K for T_{co} . However, according to Harrison *et al.*⁸³ the crossover temperature is 200 K. The saturation magnetic moment on Sm^{3+} in SmIG is $0.14 \mu_{\text{B}}$ which is much less than $0.71 \mu_{\text{B}}$,

the free ion value. This already shows the presence of crystal fields and therefore it is likely that T_{co} in M_{Sm} is also reduced to 200 K.

In conclusion, it has been shown that the mixing of ionic J levels of the Sm^{3+} ion by crystal fields and exchange fields strongly influences the temperature dependence of the 4f-susceptibility, the Knight shift of the non-magnetic site, the 4f-induced hyperfine field on the samarium nuclear site and the Sm^{3+} magnetization. In ferromagnetic samarium compounds, because of crystal fields, the Sm^{3+} ion may behave like an $(L + S)$ ion rather than an $(L - S)$ ion.

ACKNOWLEDGEMENTS

The authors are thankful to J. R. Cooper and his colleagues for making available to them the results of resistivity and specific heat measurements on $CeSn_3$.

REFERENCES

- ¹ M. A. Ruderman and C. Kittel, *Phys. Rev.* **96**, 99 (1954).
- ² T. Kasuya, *Progr. Theoret. Phys. (Kyoto)*, **16**, 45 (1956).
- ³ K. Yosida, *Phys. Rev.* **106**, 893 (1957).
- ⁴ V. Jaccarino, *J. Appl. Phys.* **32**, 102S (1961).
- ⁵ R. Vijayaraghavan, V. Udaya Shankar Rao, S. K. Malik and V. R. Marathe, *J. Appl. Phys.* **39**, 1086 (1968).
- ⁶ R. Vijayaraghavan, Satish K. Malik and V. Udaya Shankar Rao, *Phys. Rev. Letters*, **20**, 106 (1968).
- ⁷ S. K. Malik, *Ph.D. Thesis*, Bombay University (1972).
- ⁸ See for instance, H. J. van Daal and K. H. J. Buschow, *Phys. Status Solidi (a)*, **3**, 853 (1970), and references cited therein.
- ⁹ R. R. Joseph, K. A. Gschneidner Jr and R. E. Hungsberg, *Phys. Rev. B*, **5**, 1878 (1972), and references cited therein.
- ¹⁰ I. R. Harris *J. Less-Common Metals*, **14**, 459 (1968).
- ¹¹ In the results reported in refs. 5 and 6 the assignment of the n.m.r. lines to Pt_I and Pt_{II} sites and the corresponding Knight shifts and other results were inadvertently interchanged.
- ¹² K. S. V. L. Narasimhan, V. U. S. Rao and R. A. Butera, in *Magnetism and Magnetic Materials—1972*, AIP Conference Proceedings (American Institute of Physics, New York).
- ¹³ T. Tsuchida and W. E. Wallace, *J. Chem. Phys.* **43**, 3811 (1965).
- ¹⁴ G. K. Shenoy, B. D. Dunlap, G. M. Kalvius, A. M. Toxen and R. J. Gambino, *J. Appl. Phys.* **41**, 1317 (1970).
- ¹⁵ A. F. Ruggiero and G. L. Olcese, *Atti Acad. Lincei—RC Sci. Fis. Mat. Nat.* **37**, 169 (1964).
- ¹⁶ J. R. Cooper, C. Rizzuto and G. Olcese, *J. Phys., Paris*, **32**, C1-1136 (1971).
- ¹⁷ S. K. Malik and R. Vijayaraghavan, in *Proceedings of the International Conference on Magnetism, Moscow, 1973* (to be published).
- ¹⁸ I. R. Harris and G. V. Raynor, *J. Less-Common Metals*, **9**, 7 (1965).
- ¹⁹ C. R. Kanekar, K. R. P. M. Rao and V. U. S. Rao, *Phys. Letters*, **27A**, 85 (1968).
- ²⁰ V. U. S. Rao and R. Vijayaraghavan, *Phys. Letters*, **19**, 168 (1965).
- ²¹ F. Borsa, R. G. Barnes and R. A. Reese, *Phys. Status Solidi*, **19**, 359 (1967).
- ²² S. K. Malik, R. Vijayaraghavan and P. Bernier, *J. Mag. Resonance*, **8**, 159 (1972).
- ²³ W. G. Clark, *Rev. Sci. Instrum.* **35**, 316 (1964).
- ²⁴ L. B. Welsh and J. B. Darby Jr, in *Magnetism and Magnetic Materials—1972*, AIP Conference Proceedings (American Institute of Physics, New York).

- 25 S. M. Myers and A. Narath, *Solid State Commun.* **12**, 83 (1973).
- 26 B. Stalinski, Z. Kletowski and Z. Henkie, *Phys. Status Solidi* (a), **19**, K 165 (1973).
- 27 A. B. Kaiser and S. Doniach, *Internat. J. Magn.* **1**, 11 (1970).
- 28 S. Doniach and S. Engelsberg, *Phys. Rev. Letters*, **17**, 750 (1966).
- 29 P. Lederer and D. L. Mills, *Solid State Commun.* **5**, 131 (1967).
- 30 W. E. Wallace, R. S. Craig, A. Thompson, C. Deenadas, M. Dixon, M. Aoyagi and N. Marzouk, *Les Elements des Terres Rares, Coll. Int. C.N.R.S. No. 180*, 427 (1970).
- 31 B. Coqblin and A. Blandin, *Advanc. Phys.* **17**, 281 (1968) and references cited therein.
- 32 B. Coqblin and J. R. Schrieffer, *Phys. Rev.* **185**, 847 (1969).
- 33 S. DeGennaro and E. Borchì, *Phys. Rev. Letters*, **30**, 377 (1973).
- 34 S. Misawa, to appear in *Solid State Commun.*
- 35 J. H. Van Vleck, *The Theory of Electric and Magnetic Susceptibilities*. Oxford University Press: London (1932).
- 36 J. A. White and J. H. Van Vleck, *Phys. Rev. Letters*, **6**, 412 (1961).
- 37 C. Günther and I. Lindgren, in *Perturbed Angular Correlations*, edited by E. Karlsson, E. Matthias and K. Siegbahn. North Holland: Amsterdam (1964), p 355 ff., and references cited therein.
- 38 E. D. Jones and J. E. Hesse, *J. Appl. Phys.* **38**, 1159 (1967).
- 39 E. D. Jones, *Phys. Rev.* **180**, 455 (1969).
- 40 H. W. de Wijn, A. M. van Diepen and K. H. J. Buschow, *Phys. Rev.* **161**, 253 (1967).
- 41 S. K. Malik, *Phys. Letters*, **31A**, 33 (1970).
- 42 K. H. J. Buschow, A. M. van Diepen and H. W. de Wijn, *Phys. Letters*, **24A**, 536 (1967).
- 43 V. U. S. Rao, *Ph.D. Thesis*, Bombay University (1967).
- 44 S. K. Malik, R. Vijayaraghavan and P. Bernier, *J. Mag. Resonance*, **8**, 161 (1972).
- 45 S. K. Malik and R. Vijayaraghavan, *Phys. Letters*, **34A**, 67 (1971).
- 46 S. K. Malik and R. Vijayaraghavan, *J. Phys., Paris*, **32**, C1-1028 (1971).
- 47 M. T. Hutchings, in *Solid State Physics*, edited by F. Seitz and D. Turnbull. Academic Press: New York (1964), Vol. 16, p 227 ff.
- 48 K. W. H. Stevens, *Proc. Phys. Soc. (London)*, **65A**, 209 (1952).
- 49 B. Bleaney and K. W. H. Stevens, *Rep. Progr. Phys.* **16**, 108 (1953).
- 50 R. J. Elliott and K. W. H. Stevens, *Proc. Roy. Soc. (London)*, **218A**, 553 (1953).
- 51 B. R. Judd, *Proc. Roy. Soc. (London)*, **227A**, 552 (1954).
- 52 B. G. Wybourne, *Spectroscopic Properties of Rare Earths*, p 164. Wiley: New York (1965).
- 53 M. Rotenberg, R. Bivins, N. Metropolis and J. K. Wooten Jr. *The 3-j and 6-j Symbols*. MIT Press: Cambridge, Mass. (1959).
- 54 C. W. Nielson and G. F. Koster, *Spectroscopic Coefficients for p^n , d^n and f^n Configurations*. MIT Press: Cambridge, Mass. (1964).
- 55 H. W. de Wijn, A. M. van Diepen and K. H. J. Buschow, *Phys. Rev. B*, **7**, 524 (1973).
- 56 S. K. Malik, R. Vijayaraghavan, S. G. Sankar and V. U. S. Rao, to be published.
- 57 D. Shaltiel, J. H. Wernick, H. J. Williams and M. Peter, *Phys. Rev.* **135**, A1346 (1964).
- 58 S. K. Malik, unpublished.
- 59 See for instance, S. Ofer, I. Nowik and S. G. Cohen, in *Chemical Applications of Mössbauer Spectroscopy*, edited by V. I. Goldanskii and R. H. Herber, p 439. Academic Press: New York (1968).
- 60 B. R. Judd, *Operator Techniques in Atomic Spectroscopy*, p 85. McGraw-Hill: New York (1963).
- 61 Ref. 52, p 112.
- 62 S. K. Malik, presented at the Fifth International Symposium on Magnetic Resonance, Bombay, India, 1974, and to be published.
- 63 S. Ofer, E. Segal, I. Nowik, E. R. Bauminger, L. Grodzins, A. J. Freeman and M. Schieber, *Phys. Rev.* **137**, A627 (1965). These authors mention a crossover in $\langle H_z^{4f} \rangle_{av}/H$ for the free Sm^{3+} ion at 700 K. This, however, is incorrect.
- 64 S. K. Malik and R. Vijayaraghavan, to appear in *Phys. Rev. B*.
- 65 B. Bleaney, *Proc. 3rd Internat. Symp. Quantum Electronics*, p 595. Paris (1963).
- 66 P. N. Tandon, R. C. Chopra, A. P. Agnihotry, R. Vijayaraghavan and S. K. Malik, submitted for publication.
- 67 S. K. Malik and R. Vijayaraghavan, submitted for publication.

- ⁶⁸ S. K. Malik, to appear in the proceedings of the DAE Symposium on Solid State Physics and Nuclear Physics, Bangalore, India, 1973.
- ⁶⁹ S. K. Malik and R. Vijayaraghavan, submitted for publication.
- ⁷⁰ K. H. J. Buschow, A. M. van Diepen and H. W. de Wijn, *Phys. Rev. B*, **8**, 5134 (1973).
- ⁷¹ A. M. Stewart, *Phys. Status Solidi*, (b), **52**, K1 (1972).
- ⁷² W. P. Wolf and J. H. Van Vleck, *Phys. Rev.* **118**, 1490 (1960).
- ⁷³ A. M. Stewart, *Phys. Rev. B*, **6**, 1985 (1972); **8**, 2214 (1973).
- ⁷⁴ W. E. Wallace, in *Progress in the Science and Technology of the Rare Earths*, Vol. 3, edited by L. Eyring, p 1 ff. Pergamon: Oxford (1968) and references cited therein.
- ⁷⁵ W. E. Wallace, in *Progress in Solid State Chemistry*, Vol. 6, edited by H. Reiss and J. O. McCaldin, p 155 ff. Pergamon: Oxford (1971) and references cited therein.
- ⁷⁶ S. K. Malik and R. Vijayaraghavan, to be published.
- ⁷⁷ R. Pauthenet, *Ann. Phys. (Paris)*, **3**, 424 (1958).
- ⁷⁸ J. R. Cunningham and E. E. Anderson, *J. Appl. Phys.* **31**, 45S (1959).
- ⁷⁹ A. Aharoni and M. Schieber, *Phys. Rev.* **123**, 807 (1961).
- ⁸⁰ J. Perel and M. Schieber, *J. Appl. Phys. (Japan)*, **1**, 243 (1962).
- ⁸¹ C. Nowlin, *Ph.D. Thesis*, Harvard University (1963).
- ⁸² S. Geller, H. J. Williams, R. C. Sherwood, J. P. Remeika, and G. P. Espinoza, *Phys. Rev.* **131**, 1080 (1963).
- ⁸³ F. W. Harrison, J. F. A. Thompson and K. Tweedale, *Proc. Internat. Conf. Magnetism, Nottingham 1964*, p 664.